Mono(NCN-pincer palladium)-metalloporphyrin catalysts: Evidence for supramolecular bimetallic catalysis

ARTICLE *in* DALTON TRANSACTIONS · JULY 2010

Impact Factor: 4.2 · DOI: 10.1039/b925236n · Source: PubMed

6 AUTHORS, INCLUDING:

Anthony L. Spek
Utrecht University
1,591 PUBLICATIONS **55,151** CITATIONS
SEE PROFILE

Gerard van koten
Utrecht University
1,113 PUBLICATIONS **28,263** CITATIONS
SEE PROFILE

Bert Klein Gebbink
Utrecht University
238 PUBLICATIONS **4,223** CITATIONS
SEE PROFILE

Mono(NCN-pincer palladium)-metalloporphyrin catalysts: evidence for supramolecular bimetallic catalysis†

Bart M. J. M. Suijkerbuijk,[a] Daniël J. Schamhart,[a] Huub Kooijman,[b] Anthony L. Spek,[b] Gerard van Koten[a] and Robertus J. M. Klein Gebbink*[a]

Received 30th November 2009, Accepted 27th April 2010
First published as an Advance Article on the web 2nd June 2010
DOI: 10.1039/b925236n

The synthesis and catalytic properties of ditopic mono-pincer-mono-porphyrin complexes were investigated. The statistical Adler condensation reaction of 3,5-bis(methoxymethyl)-4-bromo-benzaldehyde, *p*-tolylaldehyde, and pyrrole, furnished an AB_3-type tetraphenylporphyrin, containing three *meso*-*p*-tolyl groups and one *meso*-3,5-bis(methoxymethyl)-4-bromophenyl group. This material was converted into the ditopic ligand [2H(Br)], which comprises one porphyrin site and an NCN-pincer type ligand moiety. In order to metalate this compound in a stepwise, site-selective manner, two distinct synthetic routes were followed. Route A relies on the introduction of a metal in the porphyrin cavity followed by pincer metalation and a reversal of this order is employed for route B. For the hetero-bimetallic pincer-porphyrin target compounds, route A invariably proved to be the highest yielding alternative, giving pincer-porphyrin hybrids of general formula **[M^1(M^{2}X)]** (M^1 = 2H, Mg, Co, Ni, Zn; M^2 = Pd, Br; X = Cl, Br). ^{195}Pt NMR spectroscopy revealed that the porphyrin metal has a modest influence on the electron density on the NCN-pincer Pt site. When the analogous cationic Pd complexes were used as Lewis acid catalysts for the double Michael addition between methyl vinyl ketone and ethyl α-cyanoacetate, it was noted that the catalytic activity did not depend on the central metal for M^1 = 2H, Ni, and Zn. However, when Mg occupied the porphyrin cavity, the rate of the reaction increased by a factor of six. Although a rate enhancement was observed when catalysis was conducted with a mixture of the two constituents of **[Mg(PdOH$_2$)]**BF_4 (*i.e.* MgTTP and [$PdOH_2$(NCN)]BF_4) this could not fully account for the rate enhancement. We believe that the rationale for this behaviour is dual, consisting of "cooperative dual catalysis" and supramolecular aggregation of two or more catalyst-substrate complexes.

Introduction

ECE-pincer metal complexes have found extensive application as catalysts in many organic transformations.[1–11] Their widespread use has been prompted by the ease of alteration of several key parameters of the pincer system. Chart 1 shows the general formula of such an organometallic pincer complex. It comprises an M–C_{aryl} σ-bond that is kinetically stabilised by two flanking electron-donating groups E, forming a robust organometallic complex. Depending on the chelated metal, a number of additional ligands (L) will occupy the remainder of the available coordination sites. By selecting specific combinations of M, E, and L_n, metallopincer complexes can be obtained with potential applications in research areas ranging from materials science[12–18] and catalysis[1–11,19] to sensing[20,21] and bio-marking.[22,23] As changes in these combinations greatly alter the properties of the ECE-pincer metal complexes, we have previously also investigated strategies to electronically tune the properties of a given ECE-organometallic moiety. The pincer *para*-substituent Z proved key in this respect: Van de Kuil[24] and Slagt[25,26] found that in both NCN-pincer Ni and Pt complexes, the electron density on the metal centre is proportional to the electron-withdrawing or -donating character of Z, as indexed by its Hammett parameter σ_p. Variation of the *para*-substituent on ECE-pincer metal complexes is therefore a powerful tool in the development of catalysts and materials with well-defined and fine-tuned properties.[27–30] The *para*-substituent has also been used extensively to graft and anchor pincer-metal complexes to a variety of materials and supports.[13,17,18,31–49] Alternatively, η^6-coordination

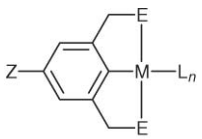

M = Li, Rh, Ru, Ni, Pd, Pt, Au
E = NR_2, OR, PR_2, SR, SeR
L = Lewis base, halide
n = 1, 2, 3
Z = *para*-substituent

Chart 1

[a]*Chemical Biology & Organic Chemistry, Debye Institute for Nanomaterials Science, Faculty of Science, Utrecht University, Padualaan 8, 3584 CH Utrecht, The Netherlands. E-mail: r.j.m.kleingebbink@uu.nl; Fax: +31-30-2523615; Tel: +31-30-2531889*
[b]*Crystal and Structural Chemistry, Bijvoet Center for Biomolecular Research, Faculty of Science, Utrecht University, Padualaan 8, 3584 CH Utrecht, The Netherlands.*

† Electronic supplementary information (ESI) available: Synthesis and analytical data for MgTTP, NiTPP and ZnTTP. CCDC reference number 755788. For ESI and crystallographic data in CIF or other electronic format see DOI: 10.1039/b925236n

of $[RuC_5R_5]^+$ fragments to the pincer phenyl ring can significantly change the properties of the pincer-born metal centre.[50–52]

Although some substituents can be directly introduced at the *para*-position of the NCN-pincer metal moiety through electrophilic aromatic substitution, most of these direct methods employ rather harsh reaction conditions.[25,53,54] In the majority of cases the introduction of a new *para*-substituent therefore involves considerable synthetic efforts. For this reason we set out to develop a modular way of changing the electronic properties of the pincer *para*-substituent using mild techniques and requiring a minimal number of synthetic steps. A modular strategy for the variation of substituents may, furthermore, be a research tool of general interest, *e.g.*, in catalyst optimization.

It has long been known that the electronic properties of a metalloporphyrin depend on the metal that is situated in its core.[55–57] This is for instance manifested in the electrochemical and photophysical properties of metalloporphyrins. During the course of a few decades, a "periodic table of metalloporphyrins" has been virtually completed and essentially any metal can be successfully introduced in the porphyrin framework.[58] Whereas in the beginning some porphyrin metalation reactions still employed rather forcing conditions, milder ways have gradually been developed to introduce particular metals with very mild methods. These beneficial aspects of porphyrin chemistry encouraged us to synthesise ECE-pincer-porphyrin hybrids and to evaluate the potential of the metalloporphyrin to act as a modular pincer *para*-substituent. In order to prevent a possible dilution of the effect of the porphyrin on the metallopincer, as might be the case when multiple metallopincer groups are attached (*cf.* the **$[M^1(M^2X)_4]$** systems studied recently),[59,60] we set out to investigate *meso*-mono(NCN-pincer metal)-(metallo)porphyrin hybrids, **$[M^1(M^2X)]$** (see Chart 2).

Here, the synthesis of the ditopic pincer-porphyrin hybrid ligand system is described along with the stepwise and orthogonal metalation of each of the ligand sites. The effect of the metalloporphyrin *para*-substituent on the electron density of the NCN-pincer metal moiety and the resulting behaviour of these compounds as homogeneous catalysts is discussed.

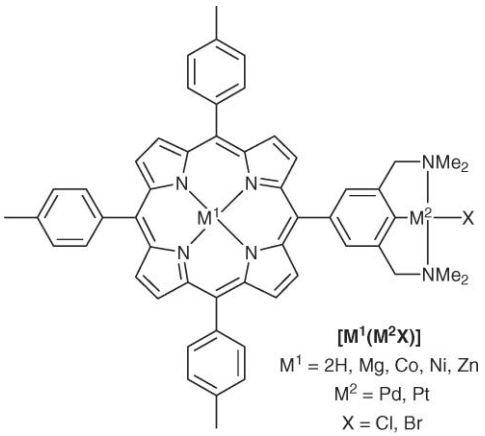

Chart 2

Synthesis and characterisation

Synthesis of the ditopic ligand

For the synthesis of the targeted mono(NCN-pincer)-porphyrin hybrid ligand **[2H(Br)]** an Adler-type condensation reaction[61] was employed, since Lindsey-type procedures were found to be less suitable in related cases.[59,62] A synthetic strategy similar to that utilised for the synthesis of the tetrakis(NCN-pincer)-porphyrin hybrids discussed in two previous papers[59,62] was used, in which a benzaldehyde with two benzylic methoxide groups at its 3- and 5-positions was employed in the porphyrin synthesis step (Scheme 1). To arrive at the desired 5-(NCN-pincer ligand)-10,15,20-tris(*p*-tolyl)-substituted porphyrin framework, a statistical condensation reaction was employed. The previously described 3,5-bis(methoxymethyl)-4-bromobenzaldehyde **1**[59] and *p*-tolualdehyde were reacted in a 1 : 5.8 molar ratio with pyrrole (6.8 equivalents) in refluxing propionic acid to give a mixture of *meso*-[3,5-bis(methoxymethyl)-4-bromophenyl]$_n$-(*p*-tolyl)$_{4-n}$ porphyrins (n = 0–4). After oxidation with DDQ in CH_2Cl_2 to remove chlorin impurities, the mixture was subjected to column chromatography on silica

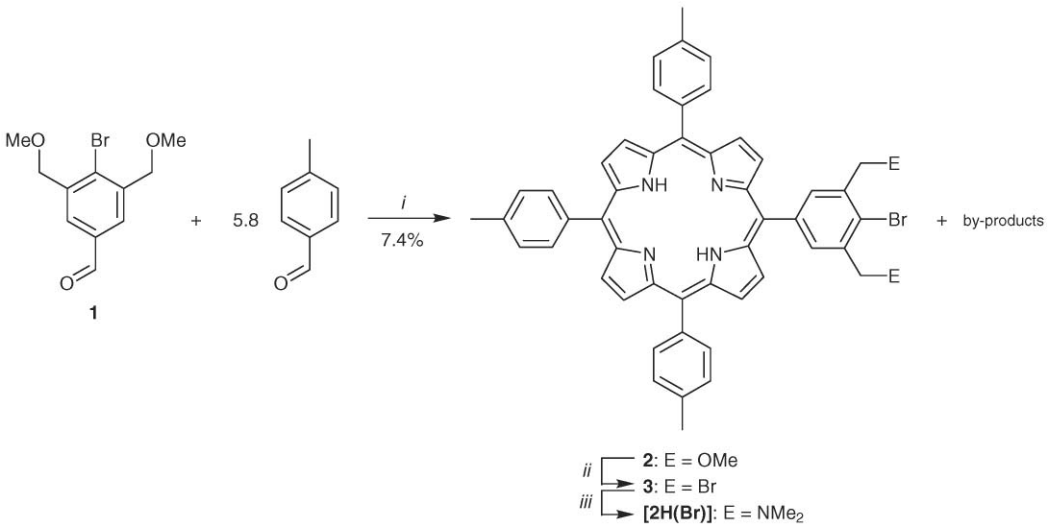

Scheme 1 Synthetic route toward **[2H(Br)]**: (i) a. pyrrole, propionic acid, reflux; b. DDQ, CH_2Cl_2; (ii) 33% HBr/HOAc, CH_2Cl_2; (iii) $HNMe_2$, CH_2Cl_2.

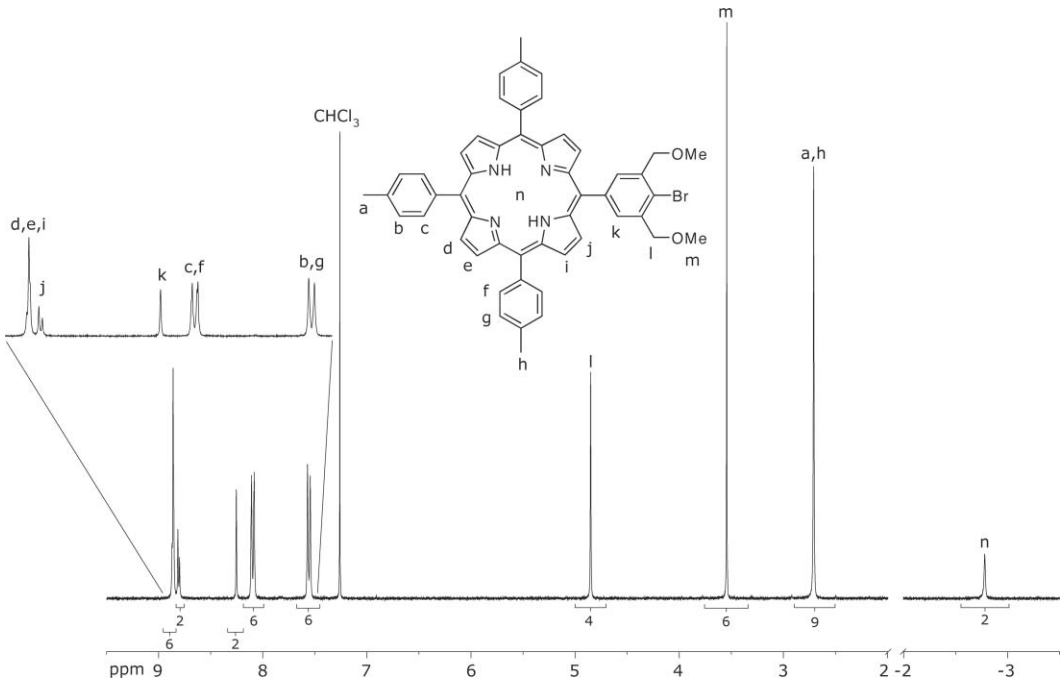

Fig. 1 ^{1}H NMR spectrum of **2** in $CDCl_3$ at 25 °C.

gel. The polarity difference of the 3,5-bis(methoxymethyl)-4-bromophenyl- and *p*-tolyl-substituents allowed for the separation of each of the porphyrin components of the mixture to give the desired 5-[3,5-bis(methoxymethyl)-4-bromophenyl]-10,15,20-tris(*p*-tolyl)porphyrin (**2**) in 7.4% yield. The by-products 5,15-bis[3,5-bis(methoxymethyl)-4-bromophenyl]-10,20-bis(*p*-tolyl)-porphyrin and *meso*-tetrakis(*p*-tolyl)porphyrin (TTP) were also isolated in 1.0% and 13% yield, respectively.

The AB_3 substitution pattern of **2** was readily apparent from its ^{1}H NMR spectrum (300 MHz), which showed three types of β-H signals (see Fig. 1). The magnetic non-equivalence of the protons at the 2- and 8-positions (Fig. 1(i)) with respect to those at the 3- and 7-positions (j) on the porphyrin ring leads to an AB-pattern at $\delta = 8.87$ and 8.81 ppm ($^{3}J_{HH} = 4.8$ Hz). On the other hand, the two sets of β-protons situated in between the two different *p*-tolyl groups (d and e) give rise to an apparent singlet at $\delta =$ 8.86 ppm. The integral ratio of the peaks corresponding to the pincer aryl-protons and the *p*-tolyl aryl-protons (2 : 12) provided further evidence for the expected one-to-three ratio and thus for the desired structure. The symmetry of the molecule was further corroborated by ^{13}C NMR spectroscopy, which typically showed three signals with approximate intensities of 1 : 2 : 1 in the C_{meso} region ($\delta \approx 120$ ppm).[63]

The effective method of HBr/HOAc treatment[62,64] was subsequently applied to convert **2** into 5-[3,5-bis(bromomethyl)-4-bromophenyl]-10,15,20-tris(*p*-tolyl)porphyrin (**3**) in 82% isolated yield (Scheme 1). When HBr/HOAc solutions containing traces of Br_2 impurity were used, β-bromination occurred to a small extent (≤6% by ^{1}H NMR). The desired ditopic ligand **[2H(Br)]** was obtained from the reaction of **3** with $HNMe_2$ in 97% yield. All compounds were fully characterised by means of ^{1}H and ^{13}C{^{1}H} NMR spectroscopy, UV-vis spectroscopy, MALDI-TOF MS, and elemental analysis (see Experimental).

Ligand metalation

In order to be able to introduce electronically diverse metals into the porphyrin skeleton that do not interfere with subsequent reactions at the pincer unit, *e.g.*, halide abstraction with $AgBF_4$ (*vide infra*), several metals were considered. It was decided to introduce relatively electronegative Co(II), electron richer Ni(II) and Zn(II), and electropositive Mg(II) in the porphyrin moiety of [2H(Br)]. For subsequent catalytic studies, the NCN-pincer Pd compounds are of interest, whereas the corresponding platinum compounds were also targeted in order to determine the electronic effects of the metalloporphyrin on the NCN-pincer metal group. To obtain the mono(NCN-metallopincer)-metalloporphyrin hybrids, two different routes can be followed, each of which consists of a two-step protocol in which first one coordination site is metalated followed by the second one. Porphyrin metalation followed by pincer metalation will be referred to as Route A, while the strategy in which the pincer site is metalated prior to porphyrin metalation is named Route B (Scheme 2). Route A proved to be superior for all targeted **[M^{1}(M^{2}X)]** compounds. Whereas the final yields for Route A were approximately 80% over two steps, Route B only furnished around 60% of the desired final product (Table 1, *vide infra*). The lower yields obtained *via* Route B are in most cases ascribed to the second step, *i.e.* porphyrin metalation in the presence of an already metalated NCN-pincer unit.

In all cases, the introduction of a metal in the porphyrin cavity of **[2H(Br)]** proceeded selectively and in high yields. Lindsey's procedure[65] to introduce Mg(II) by means of treatment with $MgBr_2{\cdot}OEt_2$ in CH_2Cl_2 in the presence of Et_3N gave **[Mg(Br)]** in 96% yield. Zinc was also routinely introduced using $Zn(OAc)_2{\cdot}2H_2O$ in a mixed solvent system of MeOH and CH_2Cl_2[66] to yield 89% of **[Zn(Br)]**. If the latter two compounds are precipitated from CH_2Cl_2 with hexanes, they form solid materials, which

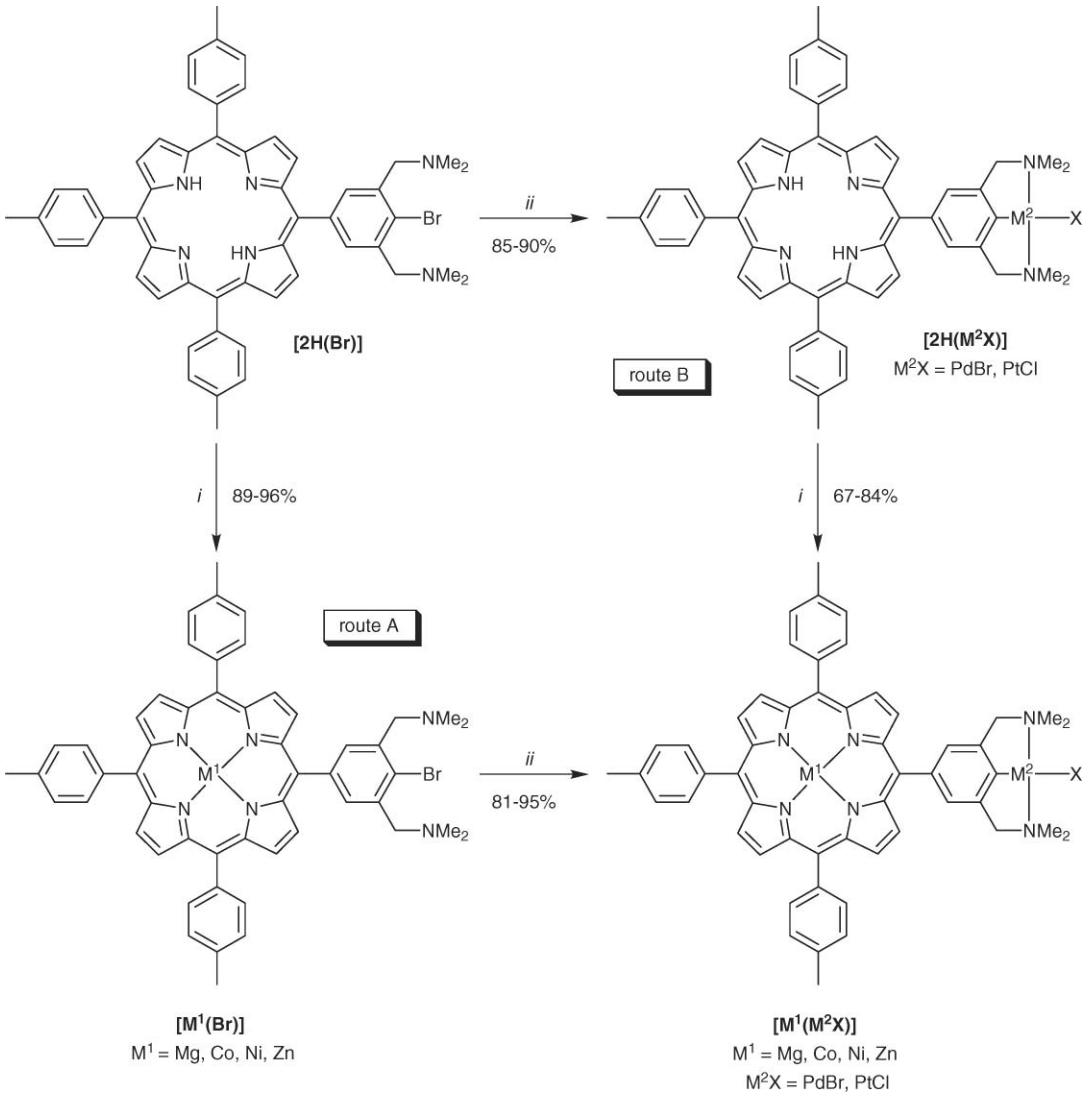

Scheme 2 Synthetic route toward bimetallic mono(NCN-pincer metal)-metalloporphyrin hybrids **[M¹(M²X)]**: (i) for M^1 = Mg: $MgBr_2{\cdot}OEt_2$, *i*-Pr_2NEt, CH_2Cl_2; for M^1 = Co: $Co(OAc)_2{\cdot}4H_2O$, MeOH–CH_2Cl_2, reflux; for M^1 = Ni: $Ni(acac)_2$, toluene, reflux, or $Ni(OAc)_2{\cdot}2H_2O$, MeOH–CH_2Cl_2; for M^1 = Zn: $Zn(OAc)_2{\cdot}2H_2O$, MeOH–CH_2Cl_2; (ii) for M^2X = PdBr: $[Pd_2dba_3]{\cdot}CHCl_3$, benzene; for M^2X = PdCl: (i) a. $[Pd_2dba_3]{\cdot}CHCl_3$, benzene; b. NaCl, H_2O–CH_2Cl_2; for M^2X = PtCl: (i) a. [Pt_2dipdba$_3$], benzene, reflux; b. $AgBF_4$, Et_3N, CH_2Cl_2; c. NaCl, H_2O–CH_2Cl_2.

Table 1 The dependence of overall yields (%) of **[M¹(M²X)]** on the synthetic route

	Route A	Route B
[Co(PdBr)]	84	N/A
[Mg(PdCl)]	84	N/A
[Ni(PdBr)]	89	66
[Zn(PdBr)]	82	76
[Mg(PtCl)]	88	61
[Ni(PtCl)]	86	57
[Zn(PtCl)]	78	61

hardly re-dissolve in non-coordinating solvents. The relatively strong interaction of magnesium[67,68] and zinc porphyrins[69] with nitrogenous bases could induce the formation of supramolecular complexes consisting of two or more **[M¹(Br)]** units (M^1 = Mg or Zn) with inherent solubility problems (see a previous publication for related *meso*-tetrakis(NCN-pincer ligand) zinc(II) porphyrins).[115] Addition of coordinating solvents such as pyridine or THF, however, leads to rapid dissolution of **[Mg(Br)]** and **[Zn(Br)]** in CH_2Cl_2 and benzene, and hexanes to a lesser extent.

In order to obtain final proof for the structure of **[Mg(Br)]** its bis(THF)-adduct {**[Mg(Br)]**$(THF)_2$} was analysed by X-ray crystallography. Dark red crystals were grown from a mixed solvent system of CH_2Cl_2/hexanes/THF (40 : 20 : 1, v/v/v) by slow concentration through evaporation of the solvents. The molecular structure shows a central Mg atom that is surrounded by six ligands in a distorted octahedral ligand arrangement (Fig. 2). Four pyrrolic nitrogen atoms provided by the porphyrin dianion occupy the meridional positions with Mg–N distances of 2.074(4)–2.077(4) Å. The two apical position are occupied by THF molecules, the oxygen atoms of which reside at 2.220(4) (O1) and 2.224(4) Å (O2) from the magnesium atom. The latter values are common for bis(oxygen) coordinated magnesium porphyrins[70] and significantly shorter than those found in the magnesium porphyrin

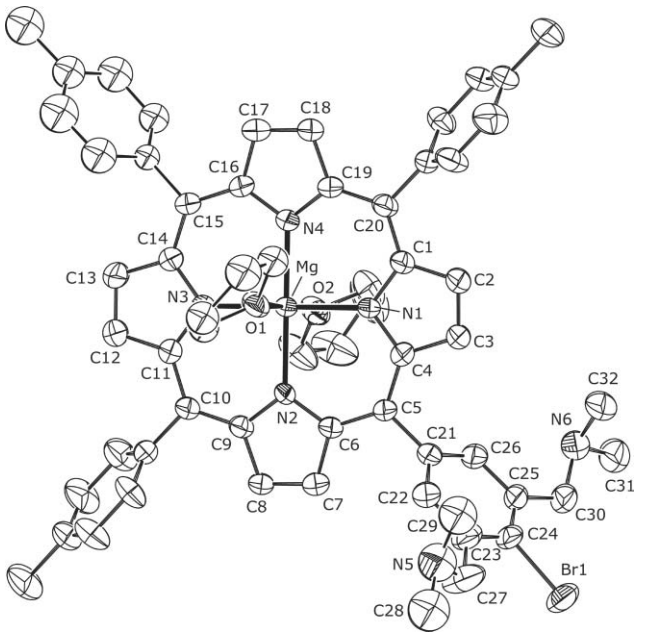

Fig. 2 Molecular structure of {**[Mg(Br)]**$(THF)_2$} with displacement ellipsoids at the 50% probability level. Hydrogen atoms and disordered non-coordinated solvent molecules have been omitted for clarity. Only one conformation of the orientationally disordered *p*-tolyl substituents is shown. Residual electron density in the proximity of C2, C3, and C12, C13, which is ascribed to partial bromination, has been left out as well.

bis-adducts of nitrogenous bases such as pyridine [2.369(2) Å][71] and *N*-methylimidazole (2.297 Å).[72]

The porphyrin macrocycle adopts a wave-type non-planar deformation mode,[73] with the N3- and N1-pyrrole rings tilted from planarity. The dihedral angles of the three *meso*-tolyl groups with respect to the central tetrapyrrolic macrocycle are between 61.0(2)° and 62.1(2)°, with the *meso*-3,5-bis[(dimethylamino)methyl]-4-bromophenyl group at 66.4(2)°. The crystallographic data furthermore show residual electron density at the positions close to C2, C3, C12, and C13. This is ascribed to a minor, partially β-brominated contamination in the starting material, which apparently co-crystallises with the major product. Besides confirming the proposed structure of **[Mg(Br)]**, this structure furthermore substantiates the AB_3 skeletal substitution pattern on the parent **[2H(Br)]** ligand and thus on all of its derivatives discussed in this paper.

Nickel(II) porphyrin **[Ni(Br)]** was synthesised in 94% by nickelation of **[2H(Br)]** with $Ni(acac)_2$ in boiling toluene. Cobalt(II) was introduced *via* treatment of **[2H(Br)]** with $Co(OAc)_2{\cdot}4H_2O$[66] in a yield of 96%. The resulting **[Co(Br)]** was obtained as a highly air- and light-sensitive solid due to the dual presence of a Co(II) centre and tertiary amine ligands within one molecule. In none of the cases, evidence was found for a competing metalation of the NCN-pincer ligand site during porphyrin metalation.

Pincer metalation

In order to metalate the pincer ligand of **[M^1(Br)]** oxidative addition of the aryl bromide moiety to M(0) precursors was chosen as the metalation method. As we observed earlier, this mild method is very selective,[59] and therefore ensures site-specific metalation, which is particularly important when the starting material is in its free-base form.

Thus, pincer palladation of all **[M^1(Br)]** compounds (M^1 = 2H, Mg, Co, Ni, Zn) proceeded smoothly with $[Pd_2dba_3]{\cdot}CHCl_3$ in benzene at room temperature to furnish the corresponding **[M^1(PdBr)]** complexes in good yields (see Table 1). During palladation of **[Mg(Br)]**, halide exchange (Br/Cl) at Pd was found to be substantial. Most probably, the chloride ions originate from residual chloroform in the starting material, which can react with pincer metal complexes to give the corresponding ECE-pincer metal chloride complexes. Hence, the **[Mg(PdX)]** product mixture (X = Br, Cl) was converted into the analogous chloridopalladio(II) compound **[Mg(PdCl)]** using NaCl as the chloride source in a biphasic system of H_2O and CH_2Cl_2.

Introduction of platinum proceeded similarly facile using 0.55 equivalents of $[Pt_2dipdba_3]$ in benzene at reflux temperature to give the corresponding **[M^1(PtBr)]** complexes (M^1 = 2H, Mg, Ni, Zn). Unlike their tetrakis(pincer) substituted analogs,[59] these complexes are sufficiently soluble in (combinations of) non-chlorinated solvents to allow for their isolation as the bromide complexes. To allow a direct comparison to the tetrapincer porphyrin complexes described previously[59] the chloride complexes seemed more relevant. Halide abstraction with $AgBF_4$ followed by treatment with brine proved to be the most effective and least time-consuming way to obtain the chloridoplatino(II) complexes. Since traces of moisture had rendered the used $AgBF_4$ acidic, the halide abstraction reactions were carried out in the presence of a base to prevent de-metalation of the metalloporphyrin. Accordingly, the desired **[M^1(PtCl)]** compounds were obtained in yields ranging from 88 to 95%.

Porphyrin metalation after pincer metalation

Notwithstanding the successful and high-yielding application of route A for the synthesis of the hetero-bimetallic compounds, it is noteworthy that for a number of compounds route B proved to be a valuable alternative. We set out to synthesise compounds **[M^1(PdBr)]** (M^1 = Ni, Zn) and **[M^1(PtCl)]** (M^1 = Mg, Ni, Zn) by porphyrin metalation of the corresponding free-base porphyrin precursors **[2H(PdBr)]** and **[2H(PtCl)]**. $Ni(acac)_2$ could not be used as a nickelating agent, since the solubility of the free-base porphyrins in toluene is too low. The use of $Ni(OAc)_2{\cdot}4H_2O$ in a mixed solvent system ($MeOH–CH_2Cl_2$)[66] led to the formation of the desired compounds, **[Ni(PdBr)]** and **[Ni(PtCl)]**, in satisfactory yields. Substantial amounts of unidentified by-product were observed in the ^{1}H NMR spectra of the crude products, but fortunately these could be readily removed by column chromatography on silica gel. Similarly, zinc(II) could be introduced using the same procedure as for **[Zn(Br)]**. **[Zn(PdBr)]** and **[Zn(PtCl)]** were thus obtained in 86 and 72% yield, respectively. Though the synthesis of **[Mg(PdCl)]** was not attempted *via* Route B, **[Mg(PtCl)]** was obtained by metalation of **[2H(PtCl)]** using Lindsey's conditions.[65] All porphyrin metalation reactions were followed by UV-vis spectroscopy. As soon as the lowest energy absorption band of the free-base porphyrin (~645 nm) had disappeared, indicating complete consumption of the starting material, the work-up was immediately performed in order to prevent product losses due to the formation of undesired by-products.

Characterisation of hetero-bimetallic compounds

All bimetallic complexes were fully characterised by a combination of ^{1}H and $^{13}C\{^{1}H\}$ NMR spectroscopy, and UV-vis spectroscopy. In addition, they were analysed by MALDI-TOF mass spectrometry and elemental analysis. In every case, the ^{1}H and $^{13}C\{^{1}H\}$ NMR spectra corroborated the AB_3 skeleton of the porphyrin. $^{13}C\{^{1}H\}$ NMR spectroscopy, for example, showed four peaks in the C_α and C_β regions[57] around δ = 150 and 131 ppm, respectively. Although not all peaks were resolved in each case, this clearly confirmed the presence of four magnetically unique C_α and C_β nuclei, which is as expected for an AB_3 porphyrin. At larger distances from the porphyrin core, these differences fade, which is illustrated by the fact that the methyl-C atoms of the two non-equivalent *p*-tolyl groups resonate at almost identical frequencies. UV-vis spectroscopy revealed that metalation of the NCN-pincer ligand moiety causes small perturbations of the electronic spectra. While metalloporphyrins **[M^1(Br)]** exhibit spectra that are virtually identical to their TTP analogues, peripheral palladation and platination bring about small bathochromic shifts of the Soret band amounting to ~1 and ~3 nm, respectively. MALDI-TOF spectra invariably showed a number of peaks corresponding to the $[M]^+$, $[M–X]^+$, and $[M–M^2X]^+$ ions. The successful incorporation of palladium and platinum was illustrated by ^{1}H NMR spectroscopy, which showed downfield shifts for the benzylic- and dimethylamino protons upon coordination of the NMe_2 groupings to the metal centre. Equally indicative were the substantial upfield shifts of the pincer aryl-protons by approximately 0.6 ppm after metalation of the NCN-pincer ligand unit. A further notable observation was that the solubility of **[Mg(M^{2}X)]** and **[Zn(M^{2}X)]** in non-coordinating solvents such as benzene and CH_2Cl_2 is dramatically enhanced in comparison with the parent metalloporphyrins. ^{1}H NMR analyses confirmed that the parent **[Mg(Br)]** and **[Zn(Br)]** compounds exist as higher order aggregates in solution due to intermolecular M–N (M = Mg or Zn) interactions, while the introduction of a metal in the pincer fragment leads to intramolecular coordination of the tertiary amines to palladium or platinum.

The platinum-containing **[M^1(PtCl)]** compounds (M^1 = 2H, Mg, Ni, Zn) were furthermore analysed by ^{195}Pt NMR spectroscopy, since it has been previously shown to be an invaluable tool for the analysis of the platinum-centred electron density in NCN-pincer platinum complexes.[25,74] Samples were measured at 2–10 mM concentrations in $CDCl_3$. It was found that for each compound the deviation of δ_{Pt} was less than 1 ppm within this concentration range. In comparison with the range of δ_{Pt} achievable by classical *para*-substitution of NCN-pincer platinum complexes (between –3236 and –2992 ppm),[25] the current span is modest (Table 2). However, these values are detectable and reproducible and, therefore, indicate a difference in the electron density at Pt as a direct consequence of a change of the porphyrin metal.

Compared to the parent [PtCl(NCN)] system, all *para*-porphyrin groups are electron donating. The obtained chemical shifts show that the electron density at Pt increases in the order M^1 = 2H < Ni < Zn < Mg. Interestingly, this order parallels the order of increasing energy of the HOMO of the respective metal complex of the corresponding tetraphenylporphyrin (TPP) complexes, *i.e.* the order of increasing ability to donate electron density.[57,75,76] The fact that the ^{195}Pt NMR resonance frequencies of a number of *para*-substituted NCN-pincer PtCl ([PtCl(NCN-Z)], Z = *para*-substituent) are known, allowed us to deduce Hammett substituent constants for the [5,10,15-tris(*p*-tolyl)porphyrinato]M^1(II) group as a whole. To this end, we used Slagt's formula (eqn (1)):[77]

$$\delta(^{195}\mathrm{Pt}) = 170.8\sigma_p - 3137.8 \quad (1)$$

Table 2 ^{195}Pt NMR chemical shifts obtained from **[M^1(PtCl)]**

	δ_{Pt}/ppm[a]	σ_p
[2H(PtCl)]	–3181	–0.25
[Ni(PtCl)]	–3183	–0.27
[Zn(PtCl)]	–3189	–0.30
[Mg(PtCl)]	–3196	–0.34
[PtCl(NCN)]	–3147	0.00

[a] Chemical shifts were referenced to an external standard (1 M $Na_2[PtCl_6]$ in D_2O) before each run.

The results are summarised in Table 2. A comparison of the values found for the classical *para*-substituted systems and the current *para*-metalloporphyrin substituted systems leads to the conclusion that, with direct C_{meso}–C_{para} bonding, the electronic influence exerted by a [5,10,15-tris(*p*-tolyl)porphyrinato]magnesium(II) group quite closely matches that of a phenolic OH group (*viz.* σ_p=–0.34 and –0.37, respectively).[78] On the other end of the spectrum, the free-base 5,10,15-tris(*p*-tolyl)porphyrin *para*-substituent comes electronically closer to a *tert*-butyl substituent.

Catalysis

NCN-pincer metal complexes have been used extensively as homogeneous catalysts for C–C coupling reactions. In this respect, the Lewis acid catalysed Michael addition of α-cyano carboxylates to alkyl vinyl ketones has been the subject of specific focus.[30,34,79–84] The relationship between the catalytic activities of several *para*-substituted NCN-pincer palladium aqua complexes [Pd(NCN-Z)OH_2]BF_4 (Z = *para*-substituent) in this reaction and the nature of the *para*-substituent was recently investigated by Van Koten *et al.*[81] They found that there is an effect of the *para*-substituent on the catalytic performance of the nearby palladium(II) centre. While the reaction is relatively slow when either an electron-donating or -withdrawing substituent is present at the *para*-position, there seems to be an optimum in the catalytic activity of the NCN-pincer palladium system when the Hammett parameter of its *para*-substituent approaches 0. Likewise, Richards found that the introduction of a *para*-nitro substituent in similar Phebox-platinum complexes led to a tenfold decrease of its activity in the same Michael addition compared to the *para*-H analog.[30] These findings prompted us to investigate the **[M^1(M^{2}X)]** hybrids complexes in the same Michael reaction.

Cationic palladium complexes

In order to use them as catalysts in the double Michael addition reaction the neutral complexes **[2H(PdBr)]**, **[Mg(PdCl)]**, **[Co(PdBr)]**, **[Ni(PdBr)]**, and **[Zn(PdBr)]** were converted into the corresponding cationic complexes **[M^1(PdOH$_2$)]**BF_4. To this end, these compounds were reacted with an excess of $AgBF_4$

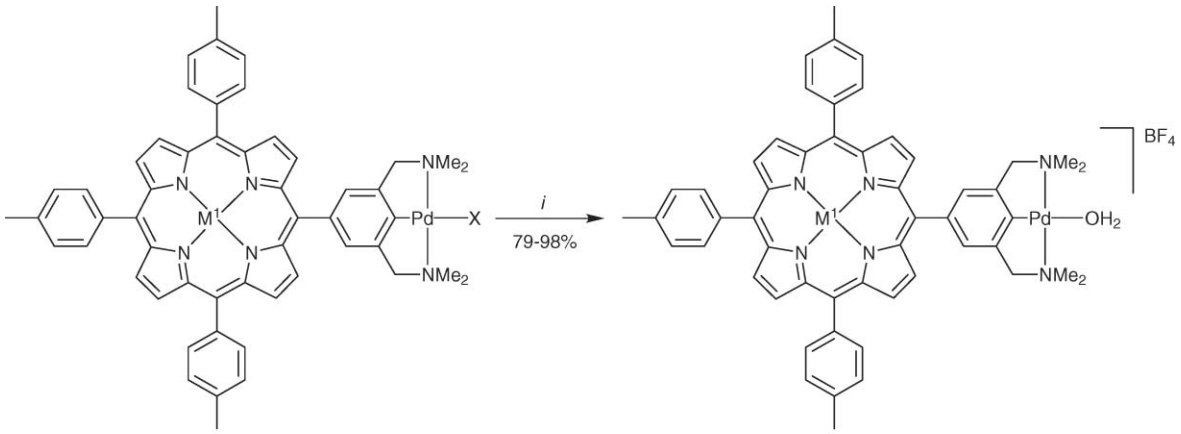

Scheme 3 Synthesis of cationic aqua complexes **[M¹(PdOH₂)]**BF_4: (i) $AgBF_4$, *i*-Pr_2NEt, CH_2Cl_2, H_2O.

(1.4–1.9 equiv.) in CH_2Cl_2 in the presence of an excess of the base *i*-Pr_2NEt (~30 equiv.) (Scheme 3).

Use of the latter was imperative since, in our case, $AgBF_4$ always seemed to contain traces of acid, which readily led to partial demetalation of the magnesium(II) and zinc(II) porphyrins. Its non-nucleophilic character further ensured that the corresponding cationic complexes could be obtained in their aqua-form. After completion of the halide abstraction, the product mixtures were filtered over Celite to remove AgX and non-dissolved $AgBF_4$. After evaporation, the filtrates were thoroughly washed with H_2O, which removed *i*-$Pr_2NEt{\cdot}HX$ and residual silver salts, and with hexanes, which eliminated any remaining *i*-Pr_2NEt. Final purification was achieved by precipitation of the desired cationic complexes from a solution in acetone/MeOH with hexanes or Et_2O. For the synthesis of **[2H(PdOH₂)]**BF_4 a slightly modified procedure without base was used, because it was envisaged that it might accelerate the introduction of silver into the porphyrin moiety. Thus, addition of $AgBF_4$ led to quick formation of a greenish reaction mixture, which, after removal of silver salts, turned red again upon addition of base. ^{1}H NMR spectroscopy confirmed the free-base identity of the porphyrin part as the signals corresponding to the pyrrolic protons at $\delta = -2.81$ ppm integrated for two with respect to the benzylic signals. Unfortunately, attempts to dehalogenate **[Co(PdBr)]** failed due to its tendency to (partially) oxidise to the corresponding Co(III) species and the synthesis of **[Co(PdOH₂)]**BF_4 was therefore abandoned.

^{1}H and ^{19}F NMR spectroscopy, and TLC analyses[85] substantiated the successful syntheses of the cationic complexes. MALDI-TOF mass spectrometry was particularly diagnostic. With 9-nitroanthracene (9NA) as matrix, the parent halidopalladio(II) complexes **[M¹(PdX)]** exhibited a strong molecular ion peak in every case (*vide supra*), in addition to the $[M–X]^+$ peak. In the cationic aqua complexes **[M¹(PdOH₂)]**BF_4, however, the signals corresponding to the halidopalladio(II) compound were completely absent, indicating a full conversion to the cationic complex. These aqua complexes were not stored prior to use, but synthesised and immediately used in the catalysis experiments.

Catalytic double Michael addition

The catalysts (0.5% Pd) were accurately weighed into a reaction flask and CH_2Cl_2 was added, leading to a suspension. Upon subsequent addition of ethyl α-cyanoacetate (CN, 1 equiv.) all solids dissolved. Methyl vinyl ketone (MVK, 3 equiv.) was added and the double Michael addition (reaction 1) was initiated by addition of Hünig's base (*i*-Pr_2NEt, 0.1 equiv.), and the reaction progress was followed by ^{1}H NMR spectroscopy.[81,86]

The catalytic results are summarised in Fig. 3 and in Table 3. The data show that the catalytic activities of **[2H(PdOH₂)]**BF_4, **[Ni(PdOH₂)]**BF_4, and **[Zn(PdOH₂)]**BF_4 are remarkably similar to that of the non-porphyrin substituted compound **[Pd(NCN)OH₂]**BF_4.[87] Apparently, the intramolecular influence of the (metallo)porphyrin on the palladium(II) centre is too small to cause significant differences. A remarkable effect, however, was observed for the magnesium(II) porphyrin-containing **[Mg(PdOH₂)]**BF_4, whose k_{obs} is more than six-fold higher than that of **[Pd(NCN)OH₂]**BF_4. Plotting $-\ln([Q]/[Q]_0)$ *vs.* time revealed that the reaction is first order in both Q = CN and Q = MVK for all catalysts.

We anticipated that a fair comparison of the performances of the pincer-porphyrin hybrids would require a determination of the catalytic activities of their (metallo)porphyrin constituents MTTP (M = 2H, Mg, Ni, Zn) (Chart 3). 2HTTP, NiTTP,[88] and ZnTTP[89] were prepared according to literature procedures and MgTTP was prepared following Lindsey's procedure for the preparation of magnesium(II) porphyrins.[65] It was found that TTP and NiTTP

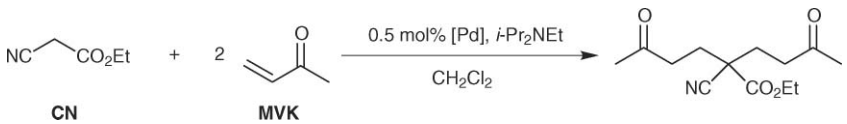

Table 3 Catalytic results of the catalysts (1.60 mM) used for the double Michael addition

Catalyst	k_{obs} ($\times 10^{-6}$ s^{-1})[a]	$t_{1/2}$/min[b]
[Pd(NCN)OH$_2$]BF$_4$	300	39
[2H(PdOH$_2$)]BF$_4$	280	41
[Mg(PdOH$_2$)]BF$_4$	1919	6
[Ni(PdOH$_2$)]BF$_4$	305	38
[Zn(PdOH$_2$)]BF$_4$	298	39
2HTTP	6	1925
MgTTP	26	444
NiTTP	6	1925
ZnTTP	7	1650
AgX (X = Br, BF$_4$)	6	1925
[PdBr(NCN)]	6	1925
Blank	6	1925

[a] Determined by ^{1}H NMR spectroscopy. The rate constant k_{obs} was determined by plotting $-\ln([CN]/[CN]_0)$ *vs.* time in seconds. [b] $t_{1/2} = \ln 2/(k \times 60)$

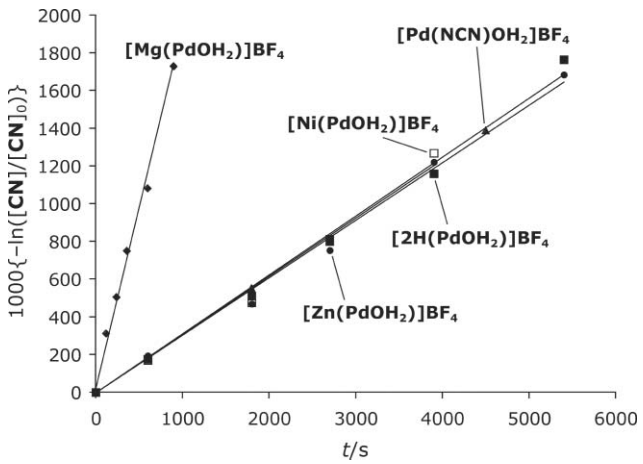

Fig. 3 Plots of $1000\{-\ln([CN]/[CN]_0)\}$ *vs.* time for cationic NCN-pincer palladium complexes.

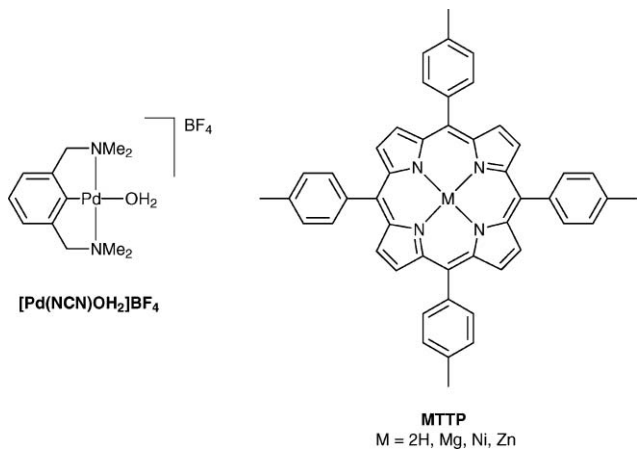

Chart 3

did not show any activity when compared to the blank reaction. However, ZnTTP showed some activity (36% conversion after 18 h compared to 28% for the blank). This is ascribed to the potential of the nitrile group of CN to coordinate to zinc(II), which also inductively renders its α-CH_2 protons more acidic. Whereas k_{obs} only increases from 6 to 7 $\times 10^{-6}$ s^{-1} (background reaction *vs.* ZnTTP-catalysed reaction), the catalytic activity of MgTTP is higher with a k_{obs} of 26×10^{-6} s^{-1}.

Table 4 Observed rate constants for different ratios of **[Pd(NCN)OH$_2$]**BF$_4$ and MgTTP

	[[Pd(NCN)OH$_2$]BF$_4$]/mM	[MgTTP]/mM	k_{obs} ($\times 10^{-6}$ s^{-1})
Entry 1	1.60	0.00	300
Entry 2	0.00	1.60	26
Entry 3	0.80	0.00	130
Entry 4	0.40	0.00	55
Entry 5	0.20	0.00	24
Entry 6	1.60	1.60	657
Entry 7	0.80	0.40	180
Entry 8	0.80	0.80	294
Entry 9	0.40	0.80	136

In order to investigate intermolecular effects in the Michael addition, several experiments involving the constituents of the pincer-porphyrin hybrids, [Pd(NCN)OH$_2$]BF$_4$ and the appropriate MTTP, were conducted. It was found that the addition of stoichiometric amounts of either 2HTTP, NiTTP, or ZnTTP to catalytic runs of [Pd(NCN)OH$_2$]BF$_4$ did not lead to appreciable effects on the rate of the reaction. However, a dramatic increase in the rate was observed when one equivalent of MgTTP was used in combination with [Pd(NCN)OH$_2$]BF$_4$: whereas k_{obs} for [Pd(NCN)OH$_2$]BF$_4$ was found to be 300×10^{-6} s^{-1}, addition of an equimolar amount of MgTTP (with respect to Pd) virtually doubled the reaction rate to $k_{obs} = 657 \times 10^{-6}$ s^{-1} (Table 4). Interestingly, this value is still a factor of three lower than that of [Mg(PdOH$_2$)]BF$_4$ itself, which indicates that its increased catalytic activity is not solely due to the arbitrary combination of the two constituents.

Next, the reaction was performed at different concentrations of [Pd(NCN)OH$_2$]BF$_4$ and MgTTP and combinations thereof. Entries 1, 3, 4 and 5 of Table 4 show that a doubling of the concentration of [Pd(NCN)OH$_2$]BF$_4$ leads to an increase in reaction rate by a factor of ~2.3, which makes the order in [Pd(NCN)OH$_2$]BF$_4$ for this reaction amounting to 1.15 in the absence of MgTTP. When MgTTP is added to the catalytic system, it functions as a co-catalyst. The addition of an equimolar amount of MgTTP leads to a 2.2 times faster reaction (*cf.* entries 1 and 6), while MgTTP itself is only a moderate catalyst (entry 2). Entries 1, 2, 7, 8 and 9 show that the overall effect of [Pd(NCN)OH$_2$]BF$_4$ on the catalytic rate is larger than that of MgTTP. With respect to entry 8, the use of half the amount of [Pd(NCN)OH$_2$]BF$_4$ leads to a rate decrease of 54% (entry 9), whereas the use of a [Pd(NCN)OH$_2$]BF$_4$/MgTTP ratio of 2/1 leads to a drop in activity of only 39% (entry 7). This is in accord with the fact that [Pd(NCN)OH$_2$]BF$_4$ itself is a better catalyst than MgTTP. However, it is clear that the rate enhancement cannot be attributed to the mere sum of the catalytic activities of the two components.

On the other hand, when the two co-catalysts are merged within one molecule, as in **[Mg(PdOH$_2$)]**BF$_4$, the situation changes dramatically. At the same total concentration of NCN-pincer palladium(II) aqua complex and magnesium(II) porphyrin, the rate of **[Mg(PdOH$_2$)]**BF$_4$ exceeds that of a 1 : 1 combination of MgTTP and [Pd(NCN)OH$_2$]BF$_4$ by a factor of three (Table 5). For example, at a concentration of 1.60 mM the rate is 1919×10^{-6} s^{-1}

Table 5 Comparison of the catalytic activities of **[Mg(PdOH$_2$)]**BF$_4$ and combinations of its components

	[**[Mg(PdOH$_2$)]**BF$_4$]/mM		k_{obs} ($\times 10^{-6}$ s^{-1})
Entry 1	1.60		1919
Entry 2	0.80		897
Entry 3	0.40		411
	[[Pd(NCN)OH$_2$]BF$_4$] (mM)	[MgTTP] (mM)	
Entry 4	1.60	1.60	657
Entry 5	0.80	0.80	294

for **[Mg(PdOH$_2$)]**BF$_4$ and 657 $\times 10^{-6}$ s^{-1} for the 1 : 1 combination of MgTTP and [Pd(NCN)OH$_2$]BF$_4$ (entry 1 *vs.* 4). At 0.80 mM, these rates have been reduced by a factor of approximately two to 897 and 294 $\times 10^{-6}$ s^{-1}, respectively (entry 2 *vs.* 5). A further reduction of the concentration of **[Mg(PdOH$_2$)]**BF$_4$ to 0.4 mM finally leads to a k_{obs} of 411 $\times 10^{-6}$ s^{-1} (entry 3). Consequently, it seems that for the three investigated concentrations, a doubling of the concentration brings about an approximate doubling in the activity. To a good approximation the reaction rate is first order in **[Mg(PdOH$_2$)]**BF$_4$, and also first order in the combination of MgTTP and [Pd(NCN)OH$_2$]BF$_4$.

After the catalytic runs, the pincer-porphyrin hybrid catalysts could be efficiently precipitated from the reaction mixtures. The addition of hexanes to the (complete) catalytic runs brought about a greater than 99.9% precipitation of the catalysts (as judged from UV-vis spectra of the hexane layer), which were isolated as their complexes with the reaction product. The re-application of these complexes as catalysts in the same double Michael addition reaction led to identical activities for at least two consecutive runs.

Discussion

Intramolecular electronic interaction

The mono(NCN-pincer metal)-metalloporphyrin hybrid complexes described here are best compared to the tetrakis(NCN-pincer metal)-metalloporphyrin hybrid complexes described earlier,[59] regarding their physical properties and, consequently, regarding the interactions between the metal sites within these complexes. The metalation of the *meso*-NCN-pincer ligands of a *tetrakis*(NCN-pincer)-metalloporphyrin causes a substantial bathochromic shift of the Soret band in the electronic spectra of the molecule ($\Delta\lambda_{max}\approx$4 nm for palladation and 12 nm for platination).[59] This was ascribed to an electronic interaction between the porphyrin and the *meso*-phenyl groups, caused by peripheral palladation or platination. Given the smaller changes of the Soret band of the present *mono*(NCN-pincer)-metalloporphyrin hybrids upon metalation of the pincer sites ($\Delta\lambda_{max}\approx$1 nm for palladation and 3 nm for platination), it seems that this effect is in fact cumulative. From preliminary ^{195}Pt NMR studies it was concluded that in the tetra-substituted systems the electronic properties of the porphyrin are passed on to the peripheral metal centres.[59] In light of the cumulative effect of the metallopincer moieties on the porphyrin core, we anticipated a potential dilution of the effects of the porphyrin on multiple NCN-pincer metal centres. As it turns out, ^{195}Pt NMR spectroscopy on these systems shows that mono-substitution of the porphyrin core does not lead to an enhanced effect of the metalloporphyrin on the NCN-pincer metal centre of the mono-systems compared to those of the *tetrakis*-systems. In fact, the δ_{Pt} range obtained for the tetra-pincer-porphyrin hybrids **[M^1(PtCl)$_4$]** seems to exceed that of the corresponding mono-pincer-porphyrin hybrids **[M^1(PtCl)]** (for M^1 = 2H, Ni, Zn), *viz.* 14 ppm for the former compared to 8 ppm for the latter. This might originate from a difference in electron-donating ability of the (metallo)porphyrin parts of these molecules.

The current research was initially aimed at intramolecularly influencing the catalytic properties of the NCN-pincer palladium centres by changing the electronic characteristics of their metalloporphyrin *para*-substituents through metalation with electronically diverse metals. When taking into account the small electronic effects exerted by the (metallo)porphyrin on the metallopincer moiety, as demonstrated by the rather small differences between the ^{195}Pt NMR chemical shifts of different **[M^1(PtCl)]** molecules, it is not surprising that the catalytic activities of **[2H(PdOH$_2$)]**BF$_4$, **[Ni(PdOH$_2$)]**BF$_4$, and **[Zn(PdOH$_2$)]**BF$_4$ are remarkably similar and virtually identical to that of [Pd(NCN)OH$_2$]BF$_4$. The significant exception to this observation is **[Mg(PdOH$_2$)]**BF$_4$, which shows a six-fold higher catalytic activity compared to the other NCN-pincer Pd complexes. The ^{195}Pt chemical shift of the related **[Mg(PtCl)]** strongly suggests that the exceedingly high activity of **[Mg(PdOH$_2$)]**BF$_4$ cannot be ascribed to intramolecular electronic effects brought about by the magnesium(II) porphyrin. The rate increase in the two-catalyst-systems consisting of [Pd(NCN)OH$_2$]BF$_4$ and MgTTP showed that, indeed, an intermolecular mechanism needs to be invoked, as the effect of MgTTP on the activity of [Pd(NCN)OH$_2$]BF$_4$ by far exceeds the expected increase in case these two metal–ligand moieties would only operate as independent catalysts.

Bimetallic catalysis

In their work on NCN-pincer M-catalysed (M = Pd, Pt) double Michael additions between α-cyano acetates and methyl vinyl ketone, Richards and co-workers showed that the catalytic mechanism of these reactions operates by virtue of coordination of the nitrogen atom of the cyano group of the substrate to the palladium atom at the position *trans* with respect to the C–M σ-bond.[79,80] This coordination event inductively lowers the pK_a of the CH$_2$ protons adjacent to the cyano group, leading to an enhanced deprotonation and reaction (Scheme 4).

During the course of the research reported here, it was found that the reaction rate of the [Pd(NCN)OH$_2$]BF$_4$-catalysed double Michael addition is first order in [CN], first order in [MVK] and approximately first order in [catalyst]. These findings indicate a transition state in which all three components are present, which is in accordance with the nucleophilic attack of the transient palladium-coordinated cyano enolate on the α,β-unsaturated ketone MVK (Scheme 4, TS 1). The order in [Pd(NCN)OH$_2$]BF$_4$ deviates somewhat from 1 (~1.15), which shows that more than one catalytic mechanism is operative. This might indicate that, in addition to activating the cyano substrate, the palladium catalyst is also capable of activating the MVK towards nucleophilic attack (*vide infra*), albeit to a smaller extent. It was also found that MgTTP catalyses the double Michael addition reaction, albeit with a rather low reaction rate (*cf.* k_{obs} is 26 $\times 10^{-6}$ s^{-1} compared

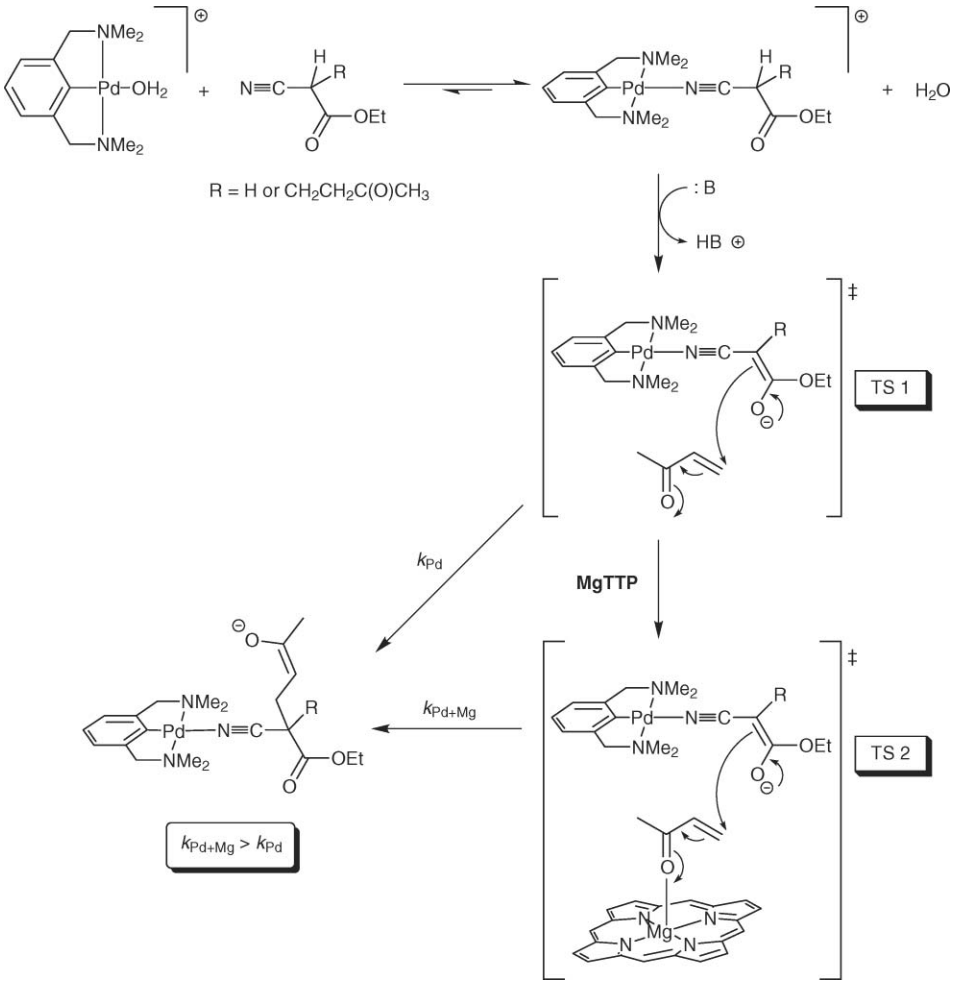

Scheme 4 Proposed mechanisms and transition states for the catalysed Michael addition reaction (R = H or $CH_2CH_2C(O)CH_3$). The porphyrin substituents have been omitted for clarity.

to 300×10^{-6} s^{-1} for $[Pd(NCN)OH_2]BF_4$). The catalytic effect of MgTTP is probably caused by coordination of either of the substrates to the magnesium centre.

The observed rate increase upon combining MgTTP and $[Pd(NCN)OH_2]BF_4$ in a co-catalytic mixture might be explained by the well-known ability of Lewis acids to catalyse Michael additions *via* coordination to, and concomitant activation of, Michael acceptor systems.[90] For the co-catalytic set-up, we propose that MgTTP enhances the rate of reaction through activation of MVK toward nucleophilic attack by coordination to its carbonyl oxygen atom through its hard magnesium atom (Scheme 4, TS 2). It should be noted, however, that due to the substantial catalytic activity of $[Pd(NCN)OH_2]BF_4$ both the palladium-catalysed reaction and the co-catalytic reaction are likely operating simultaneously and each contribute to the overall reaction rate.

Similar co-catalytic behaviour has been observed before, for instance by Ito and co-workers. They showed that nitriles, which are activated by coordination to rhodium, can be alkylated by using the ability of a co-catalytic palladium complex to generate electrophilic η^3-allyl species from allylic carbonates.[91] A related effect was exploited by Jacobsen *et al.* in an enantioselective conjugate cyanation of unsatured imides.[92] In what was coined as "cooperative dual catalysis", they used a combination of a (salen)Al μ-oxo dimer and a (pybox)$YbCl_3$ complex to greatly increase the rate and enantioselectivity of the reaction with respect to the rates achieved by either of the two catalysts independently. Recently, Peters *et al.* described the elegant use of a bis(palladium complex) ferrocene as a bimetallic catalyst for highly enantioselective Michael additions between α-cyano-aryl-acetates and methyl vinyl ketone.[93] They attribute activation of methyl vinyl ketone to coordination of its C=C bond to the soft Pd.

The one-to-one merger of MgTTP and $[Pd(NCN)OH_2]BF_4$ into one molecule, *i.e.* into **$[Mg(PdOH_2)]BF_4$**, leads to a three-fold increase of its catalytic activity compared to that found for a 1 : 1 mixture of its constituents. Molecular modelling studies showed that the enhanced performance cannot be explained by the classical effect of bimetallic catalysis, *i.e.* wherein two intramolecular metal sites cooperate directly.[93–96] The distance between a palladium-coordinated CN carbanion and a magnesium-coordinated MVK reactant within the same pincer-porphyrin unit would be simply too large for a direct reaction to occur. Since the two substrates cannot react with each other intramolecularly, a rationale for the rate enhancement has to be based on intermolecular arguments.

With an initial 200-fold excess of CN and a 600-fold excess of MVK it is plausible to assume that the pincer-porphyrin hybrids exist as fully substrate-coordinated species. The CN nitrile is coordinated to palladium while the magnesium(II) ions are coordinated to the MVK carbonyl atom. When the C_α position of the coordinated CN group is deprotonated, each catalyst-substrate complex contains two activated substrate species. The moment two such perligated molecules approach each other, the first Michael addition is intermolecular. The occurrence of this reaction at the same time interconnects the two pincer-porphyrin hybrids *via* two coordination bonds (Mg–O and Pd–N bonds), making the second Michael addition on the opposite site of the complex an intramolecular reaction, which would lead to a rate enhancement. Several such mechanisms can be proposed. However, more experimental evidence will be needed to formulate a definitive model explaining the observed catalytic rate enhancement.

Finally, it is worthwhile to discuss the differences between the similar zinc(II) and magnesium(II) porphyrins, since, unlike their magnesium(II) relatives, none of the catalyst(-mixtures) containing ZnTTP or **[Zn(PdOH$_2$)]**BF$_4$ showed a significant increase in activity. While their sizes are similar, zinc(II) is considered to be a "softer" metal than magnesium(II).[97,98] In a number of cases, this has led to intricate differences between their reactivities in identical ligand systems.[99,100] Being a hard ion, magnesium(II) prefers to bind to hard oxygen-containing ligands such as carbonyls,[101,102] while the interaction of zinc(II) porphyrins with ketones is known to be extremely weak.[103] For the current situation, these findings lead to the much stronger coordination of MVK to magnesium compared to zinc,[104] which would lead to a more efficient activation of MVK. Based on the hard–soft acid–based (HSAB) concept, it is expected that MVK is activated by coordination of its oxygen atom to magnesium rather than by its C=C double bond to Pd, which is the rationale put forward by Peters *et al.* for their systems.[93]

Conclusions

A series of hetero-bimetallic mono-pincer-porphyrin hybrids have been synthesised in excellent yields. Two routes were employed to arrive at these compounds, namely route A, in which the porphyrin is metalated prior to pincer metalation and route B, in which the latter precedes the former. In all cases, route A proved to be the highest yielding, although it sacrifices the modular approach of the synthesis route to a certain extent. In accordance with ^{195}Pt NMR measurements on **[M^1(PtCl)]** (M^1 = 2H, Mg, Ni, Zn), which did not show a strong influence of the metalloporphyrin pincer-*para* substituent on the electron density at the Pt centre, the catalytic activities of the corresponding cationic palladium complexes **[M^1(PdOH$_2$)]**BF$_4$ (M^1 = 2H, Ni, Zn) in the double Michael reaction of ethyl α-cyanoacetate with methyl vinyl ketone turned out to be very similar and comparable to the value found for [Pd(NCN)OH$_2$]BF$_4$. To genuinely promote a through-bond influence of the porphyrin on the pincer, several times greater than the ones we observe in the current systems, it is advisable to introduce a spacer in between the two constituents that allows for co-planarity of the two attached π-systems. In this respect, the ethyn-diyl spacer has proven to be highly promising in related systems.[105–107]

Surprisingly, however, the magnesium-palladium hybrid **[Mg(PdOH$_2$)]**BF$_4$ catalysed the double Michael reaction six times faster than all other hybrids. Control experiments showed that this observation could partially be attributed to the activating effect of the magnesium(II) porphyrin moiety on MVK, which leads to a cooperative dual catalysis mechanism in which the CN-substrate is activated by the pincer-Pd fragment while the magnesium porphyrin activates the MVK substrate. To fully account for the enhanced activity of **[Mg(PdOH$_2$)]**BF$_4$, though, a supramolecular mechanism has been proposed. To the best of our knowledge, this is one of the first examples in which such supramolecular catalysis behaviour is operative. It shows the promising application of the concept of "cooperative dual catalysis" but also underlines the possibility of enhancing the catalytic properties of these systems even further by merging or interconnecting the collaborating catalysts.

Experimental

General

Unless stated otherwise, all reactions were performed under a dry, oxygen-free, nitrogen atmosphere using standard Schlenk techniques and were shielded from ambient light using aluminium foil. Et_2O and THF were carefully dried and distilled from sodium/benzophenone prior to use, while CH_2Cl_2, Et_3N, and *i*-Pr_2NEt were distilled from CaH_2. Pyrrole was distilled from CaH_2 and stored under a nitrogen atmosphere at −30 °C. Methyl vinyl ketone and ethyl α-cyanoacetate were each distilled three times prior to use. All solvents and liquid reagents were thoroughly deoxygenated with a steady stream of nitrogen for at least 20 min before storage or use. 3,5-Bis(methoxymethyl)-4-bromobenzaldehyde (**1**),[59] [Pd$_2$dba$_3$]·CHCl$_3$,[108] and [Pt$_2$dipdba$_3$][109] were synthesised according to literature procedures. The syntheses of MgTTP, NiTTP and ZnTTP are described in the electronic supplementary information. Column chromatography was performed using ACROS silica gel for column chromatography, 0.060–0.200 mm, pore diameter *ca.* 6 nm or Merck Aluminium oxide 90, active basic (0.063–0.200 mm). ^{1}H and ^{13}C{^{1}H} NMR spectra were recorded at 300 MHz and 75 MHz, respectively, on a Varian 300 spectrometer operating at 298 K, and were referenced to residual solvent signal. *J* values are given in Hz. The ^{13}C NMR signals for the free-base porphyrin α- and β-carbon atoms were not resolved due to extreme line-broadening.[110] UV-vis spectra were recorded on a Cary 50 scan UV-visible spectrophotometer. MALDI-TOF measurements were performed on an Applied Biosystems Voyager-DE PRO biospectrometry workstation with either 9-nitroanthracene (9NA) or 2,5-dihydroxybenzoic acid (DHB) as the matrix, or without matrix (LDI); ESI-MS measurements were performed at the Biomolecular Mass Spectrometry Group, Bijvoet Centre for Biomolecular Research, Utrecht University, the Netherlands. Elemental microanalyses were performed by Dornis und Kolbe, Mikroanalytisches Laboratorium, Müllheim a/d Ruhr, Germany.

5-[3,5-Bis(methoxymethyl)-4-bromophenyl]-10,15,20-tris(*p*-tolyl)porphyrin (2)

Freshly distilled pyrrole (14.1 mL, 203 mmol) was added during 1 min to a colourless, refluxing solution of 3,5-bis(methoxymethyl)-4-bromobenzaldehyde **1** (7.91 g, 29.0 mmol)

and *p*-tolualdehyde (20.6 mL, 174 mmol) in propionic acid (200 mL). The solution immediately darkened, eventually turning black, and reflux was maintained for a further 35 min under air. The solution was allowed to cool down to room temperature overnight, after which the purple microcrystalline precipitate was filtered off and washed with MeOH until the washings were colourless. The residue was dissolved in CH_2Cl_2 (1.1 L), treated with DDQ (300 mg, 1.32 mmol) and the resulting orange mixture was stirred at ambient temperature for 30 min. The mixture was loaded onto a silica gel column, which was prepared with hexanes/CH_2Cl_2 (1 : 1, v/v). The first band was eluted with hexanes/CH_2Cl_2 (1 : 1 → 1 : 5, v/v) and the volatiles were evaporated to give TTP (3.71 g, 13%) as a purple, crystalline solid. LDI-TOF MS: *m/z* 671.61 ([M + H]$^+$), calcd for $C_{48}H_{39}N_4$: 671.32. The second band containing **2** was eluted with hexanes/CH_2Cl_2 (1 : 5, v/v) and CH_2Cl_2–THF (19 : 1, v/v). The volatiles were concentrated to 10 mL and MeOH (80 mL) was added at once to induce precipitation of **2** as a purple, fluffy solid (1.78 g, 7.4%), which was collected by centrifugation. Found: C 74.24, H 5.20, N 6.71. Calcd for $C_{51}H_{43}BrN_4O_2$: C 74.36, H 5.26, N 6.80%; $\lambda_{max}(CH_2Cl_2)$/nm 419 (log ε 5.72), 516 (4.30), 553 (4.04), 594 (3.77), 646 (3.77); $\delta_H(CDCl_3)$ 8.87 (6 H, m, β-H), 8.81 (2 H, d, *J* 4.8, β-H), 8.25 (2 H, s, ArH_{pincer}), 8.09 (6 H, d, *J* 7.8, Ar$H_{p\text{-tol}}$), 7.56 (6 H, d, *J* 7.8, Ar$H_{p\text{-tol}}$), 4.85 (4 H, s, CH_2O), 3.54 (6 H, s, OCH_3), 2.71 (9 H, s, ArCH_3), –2.78 (2 H, s, N*H*); $\delta_C(CDCl_3)$ 141.6, 139.5, 139.4, 137.6, 136.5, 134.7, 134.2, 127.6, 123.1, 120.7, 120.5, 118.6, 74.6, 59.0, 21.7; ESI-MS: *m/z* 825.11 ([M + H]$^+$. $C_{51}H_{44}BrN_4O_2$ requires 825.26).

5-[3,5-Bis(bromomethyl)-4-bromophenyl]-10,15,20-tris(*p*-tolyl)porphyrin (3)

A suspension of **2** (483 mg, 586 μmol) in CH_2Cl_2 (43 mL) was treated with HBr/HOAc (185 mL) and the resulting green solution was stirred for 4.5 h at room temperature. Ice water was added and after 10 min, the layers were separated. The organic layer was washed with H_2O (100 mL) and 4 M K_2CO_3 (2 × 100 mL) (the organic layer now turned red), dried ($MgSO_4$), filtered, and concentrated to 40 mL. The red solution was loaded onto a silica gel column, and the desired product was eluted as the first red band with CH_2Cl_2–hexane (1 : 1, v/v). This band was collected, evaporated to 20 mL and hexane was added to induce precipitation of the title compound as a purple solid. Yield: 439 mg (82%). Found: C 63.74, H 4.12, N 5.96. Calcd for $C_{49}H_{37}Br_3N_4$: C 63.86, H 4.06, N 6.08%; $\lambda_{max}(CH_2Cl_2)$/nm 420 (log ε 5.71), 516 (4.32), 553 (4.00), 592 (3.82), 647 (3.74); $\delta_H(CDCl_3)$ 8.92 (2 H, d, *J* 4.8, β-H), 8.87 (4 H, s, β-H), 8.80 (2 H, d, *J* 4.8, β-H), 8.28 (2 H, s, ArH_{pincer}), 8.09 (6 H, d, *J* 7.8, Ar$H_{p\text{-tol}}$), 7.56 (6 H, d, *J* 7.8, Ar$H_{p\text{-tol}}$), 4.92 (4 H, s, CH_2Br), 2.71 (9 H, s, ArCH_3), –2.79 (2 H, s, N*H*); $\delta_C(CDCl_3)$ 142.6, 139.3, 139.2, 137.6, 137.5, 137.1, 137.0, 134.6, 127.6, 126.4, 121.0, 120.7, 116.5, 34.1, 21.7; MALDI-TOF MS (DHB): *m/z* 923.01 ([M + H]$^+$. $C_{49}H_{38}Br_3N_4$ requires 923.05).

5-(3,5-Bis[(dimethylamino)methyl]-4-bromophenyl)-10,15,20-tris(*p*-tolyl)porphyrin ([2H(Br)])

A dark red solution of **3** (288 mg, 312 μmol) in CH_2Cl_2 (40 mL) was treated with Me_2NH (0.5 mL, excess) at room temperature and the solution was stirred for 3 h. Degassed H_2O (40 mL) was added and after 3 h of vigorous stirring, the layers were separated and the organic layer was dried ($MgSO_4$), filtered and concentrated with MeOH (100 mL) to 40 mL. The product was isolated as a purple solid. Yield: 258 mg (97%). Found: C 74.83, H 5.75, N 9.80. Calcd for $C_{53}H_{49}BrN_6$: C 74.90, H 5.81, N 9.89%; $\lambda_{max}(CH_2Cl_2)$/nm 419 (log ε 5.88), 517 (4.49), 552 (4.19), 592 (3.99), 648 (3.89); $\delta_H(CDCl_3)$ 8.88 (6 H, m, β-H), 8.81 (2 H, d, *J* 4.8, β-H), 8.19 (2 H, s, ArH_{pincer}), 8.10 (6 H, d, *J* 7.8, Ar$H_{p\text{-tol}}$), 7.56 (6 H, d, *J* 7.8, Ar$H_{p\text{-tol}}$), 3.84 (4 H, s, CH_2N), 2.71 (9 H, s, ArCH_3), 2.43 (12 H, s, N(CH_3)$_2$), –2.77 (2 H, s, N*H*); $\delta_C(CDCl_3)$ 140.9, 139.4, 139.4, 137.5, 137.3, 135.6, 134.6, 127.6, 127.2, 120.5, 120.4, 118.8, 64.4, 46.0, 21.7; MALDI-TOF MS (DHB): *m/z* 849.86 ([M + H]$^+$. $C_{53}H_{49}BrN_6$ requires 825.26).

5-(3,5-Bis[(dimethylamino)methyl]-4-bromidopalladio(II)-phenyl)-10,15,20-tris(*p*-tolyl)porphyrin ([2H(PdBr)])

[2H(Br)] (37 mg, 44 μmol) was dissolved in dry benzene (10 mL), $[Pd_2dba_3]\cdot CHCl_3$ (25 mg, 24 μmol) was added, and the dark red solution stirred at ambient temperature for 16 h. MeOH (0.2 mL) and Et_2NH (0.2 mL) were then added and after three hours, the mixture was filtered over Celite and the residue was washed with benzene/acetone (1 : 1, v/v, 20 mL). The red filtrate was concentrated to 5 mL and hexanes (80 mL) were added to precipitate the product **[2H(PdBr)]** as a purple solid, which was isolated by centrifugation. Possible dba contamination can be washed away with hexanes. Yield: 38 mg (90%). Found: C 66.48, H 5.04, N 8.71. Calcd for $C_{53}H_{49}BrN_6Pd$: C 66.56, H 5.16, N 8.79%; $\lambda_{max}(CH_2Cl_2)$/nm 421 (log ε 5.79), 517 (4.37), 554 (4.13), 595 (3.83), 651 (3.78); $\delta_H(CDCl_3)$ 8.85 (8 H, m, β-H), 8.09 (6 H, d, *J* 7.8, Ar$H_{p\text{-tol}}$), 7.59 (2 H, s, ArH_{pincer}), 7.54 (6 H, d, *J* 7.8, Ar$H_{p\text{-tol}}$), 4.24 (4 H, s, CH_2N), 3.17 (12 H, s, N(CH_3)$_2$), 2.71 (9 H, s, ArCH_3), –2.77 (2 H, s, N*H*); $\delta_C(CDCl_3)$ 157.0, 143.3, 139.3, 139.0, 137.5, 137.5, 134.6, 131.2 (br), 127.6, 126.3, 120.4, 120.3, 120.1, 74.8, 54.0, 31.1; MALDI-TOF MS (DHB): *m/z* 957.09 ([M + H]$^+$. $C_{53}H_{50}BrN_6Pd$ requires 956.34), 874.97 ([M – Br]$^+$. $C_{53}H_{49}N_6Pd$ requires 875.31), 769.77 ([M – PdBr]$^+$. $C_{53}H_{50}N_6$ requires 769.40).

[5-(3,5-Bis[(dimethylamino)methyl]-4-bromophenyl)-10,15,20-tris(*p*-tolyl)porphyrinato]-magnesium(II) ([Mg(Br)])

Magnesium was introduced by stirring a solution of **[2H(Br)]** (102 mg, 120 μmol) in a mixture of CH_2Cl_2 (10 mL) and Et_3N (1 mL) with $MgBr_2\cdot OEt_2$ (668 mg, 2.59 mmol) at room temperature for 15 min. All volatiles were subsequently evaporated and the residue was suspended in CH_2Cl_2 and loaded onto an alumina column. Elution with Et_3N/CH_2Cl_2 (1 : 200, v/v) gave residual starting material, whereas the desired product was eluted with THF–CH_2Cl_2 (1 : 10, v/v). The product-containing band was evaporated to dryness, toluene was added and the mixture was evaporated to dryness once again. The remaining solid was taken up in CH_2Cl_2 (40 mL) and washed with H_2O (2 × 60 mL), K_2CO_3 (0.5 M, 2 × 60 mL), and brine (50 mL). The organic layer was dried ($MgSO_4$), filtered and concentrated to 5 mL. Hexanes (50 mL) were added, the mixture was concentrated to 30 mL) and the precipitated blue/greenish solid was collected by centrifugation and dried *in vacuo*. Yield: 100 mg (96%). Found: C 66.90, H 6.85, N 6.87. Calcd for $C_{67}H_{83}BrCl_2MgN_6O_3$ ($C_{53}H_{47}BrMgN_6\cdot CH_2Cl_2\cdot 3H_2O\cdot 2C_6H_{14}$): C 67.31, H 7.00, N 7.03%; $\lambda_{max}(CH_2Cl_2)$/nm 427 (log ε 5.84), 565 (4.33), 605 (4.11); $\delta_H(CDCl_3$/1% pyridine-d_5) 8.87 (6 H, m, β-H),

8.81 (2 H, d, *J* 4.4, β-H), 8.15 (2 H, s, ArH_{pincer}), 8.07 (6 H, d, *J* 7.6, Ar$H_{p\text{-tol}}$), 7.51 (6 H, d, *J* 7.6, Ar$H_{p\text{-tol}}$), 3.81 (4 H, s, CH_2N), 2.69 (9 H, s, ArCH_3), 2.41 (12 H, s, N(CH_3)$_2$); δ_C($CDCl_3$/1% pyridine-d_5) 150.3, 150.3, 150.0, 142.6, 141.1, 136.8, 136.7, 136.0, 134.8, 134.8, 132.2, 132.0, 132.0, 131.5, 127.2, 126.8, 122.1, 121.9, 120.3, 64.5, 46.0, 21.7; LDI-TOF MS: *m*/*z* 872.31 (M^+. $C_{53}H_{47}BrMgN_6$ requires 872.29).

[5-(3,5-Bis[(dimethylamino)methyl]-4-chloridopalladio(II)-phenyl)-10,15,20-tris(*p*-tolyl)porphyrinato]magnesium(II) ([Mg(PdCl)])

$[Pd_2dba_3]\cdot CHCl_3$ (48 mg, 46 μmol) and **[Mg(Br)]** (60 mg, 69 μmol) were weighed into a flame-dried Schlenk and dry benzene (30 mL) was added, yielding a reddish suspension. Dry THF (2 mL) was added whereupon all solids dissolved, and the solution was stirred for 3 h at room temperature. Et_2NH (100 μL) and MeOH (100 μL) were then added and after an additional 2 h of stirring, the mixture was filtered over Celite and the residue was washed with acetone. All volatiles were evaporated and the resulting purple solid was stirred overnight in a mixture of CH_2Cl_2 (10 mL) and brine (10 mL). The organic layer was isolated, dried ($MgSO_4$), filtered, and concentrated to 5 mL. Upon addition of hexanes (80 mL) the desired product precipitated as a greenish solid, which was isolated by centrifugation and dried *in vacuo*. Yield: 59 mg (88%). Found: C 67.93, H 5.05, N 8.78. Calcd for $C_{53}H_{47}ClMgN_6Pd$: C 68.14, H 5.07, N 9.00%; λ_{max}(CH_2Cl_2)/nm 426 (log ε 5.84), 566 (4.39), 606 (4.20); δ_H($CDCl_3$/1% pyridine-d_5) 8.87 (8 H, m, β-H), 8.06 (6 H, m, Ar$H_{p\text{-tol}}$), 7.58 (2 H, s, ArH_{pincer}), 7.50 (6 H, m, Ar$H_{p\text{-tol}}$), 4.20 (4 H, s, CH_2N), 3.11 (12 H, s, N(CH_3)$_2$), 2.69 (6 H, s, ArCH_3), 2.67 (3 H, s, ArCH_3); δ_C($CDCl_3$/1% pyridine-d_5) 155.4, 150.4, 150.3, 150.2, 150.1, 142.8, 141.1, 140.7, 136.8, 134.8, 132.0, 131.9, 131.7, 127.2, 126.6, 121.9, 121.8, 121.7, 75.1, 53.5, 21.7; MALDI-TOF MS (9NA): *m*/*z* 934.63 ($[M]^+$. $C_{53}H_{47}ClMgN_6Pd$ requires 934.25), 897.53 ($[M - Cl]^+$. $C_{53}H_{47}MgN_6Pd$ requires 897.54), 791.29 ($[M - PdCl]^+$. $C_{53}H_{47}MgN_6$ requires 791.37).

[5-(3,5-Bis[(dimethylamino)methyl]-4-bromophenyl)-10,15,20-tris(*p*-tolyl)porphyrinato]cobalt(II) ([Co(Br)])

A dark red solution of **[2H(Br)]** (60.2 mg, 70.8 μmol) in CH_2Cl_2 (30 mL) was stirred at room temperature and a dark red solution of $Co(OAc)_2\cdot 4H_2O$ (600 mg, 2.41 mmol) in hot MeOH (10 mL) was added. The solution was subsequently heated to reflux for 2 h and then stirred at ambient temperature for 12 h. The red suspension was washed with $NaHCO_3$ (5% in H_2O, 3 × 50 mL), H_2O (3 × 50 mL), brine (50 mL), dried ($MgSO_4$), and filtered. The clear, red filtrate was concentrated to dryness and stored *in vacuo* to give the title complex as a bright red solid. Yield: 61.8 mg (96%). Because of its instability, this compound was immediately used in the following step. λ_{max}(CH_2Cl_2)/nm 412 (relative intensity 1.000), 529 (0.058); MALDI-TOF MS (DHB): *m*/*z* 907.43 ($[M + H]^+$. $C_{53}H_{48}BrN_6Co$ requires 907.24).

[5-(3,5-Bis[(dimethylamino)methyl]-4-bromidopalladio(II)-phenyl)-10,15,20-tris(*p*-tolyl)porphyrinato]-cobalt(II) ([Co(PdBr)])

[Co(Br)] (60.8 mg, 67.2 μmol) was dissolved in benzene (20 mL) followed by $[Pd_2dba_3]\cdot CHCl_3$ (40.0 mg, 38.6 μmol) and the resulting dark solution was stirred during 48 h at ambient temperature. THF (3 mL) was subsequently added, followed by Et_2NH (2 drops) after 2 h. After a further 3 h, all volatiles were evaporated *in vacuo* and the red residue was redissolved in benzene (20 mL) and filtered through Celite. The filtrate was concentrated to dryness and the resulting solid was washed with pentane (3 × 50 mL) to give a red solid. Yield: 55.2 mg (81%). λ_{max}(CH_2Cl_2)/nm 413 (relative intensity 1.000), 530 (0.060); δ_H($CDCl_3$) 15.91 (8 H, br, β-H), 13.06 (6 H, br, Ar$H_{p\text{-tol}}$), 12.57 (2 H, br, ArH_{pincer}), 9.74 (6 H, br, Ar$H_{p\text{-tol}}$), 5.47 (4 H, s, CH_2N), 4.16 (6 H, s, ArCH_3), 4.13 (3 H, s, ArCH_3), 4.07 (12 H, s, N(CH_3)$_2$); due to extreme line broadening a ^{13}C spectrum could not be recorded; MALDI-TOF MS (9NA): *m*/*z* 1013.73 ($[M]^+$. $C_{53}H_{47}BrCoN_6Pd$ requires 1013.14), 932.51 ($[M - Br]^+$. $C_{53}H_{47}CoN_6Pd$ requires 932.23),

[5-(3,5-Bis[(dimethylamino)methyl]-4-bromophenyl)-10,15,20-tris(*p*-tolyl)porphyrinato]nickel(II) ([Ni(Br)])

[2H(Br)] (23 mg, 27 μmol) and $Ni(acac)_2$ (0.16 g, 623 μmol) were suspended in dry toluene and the mixture was heated to reflux for 2 h. All volatiles were subsequently evaporated *in vacuo* and the remaining orange solid was dissolved in CH_2Cl_2 (20 mL) and washed with 5% K_2CO_3 (4 × 40 mL). The organic layer was isolated, dried ($MgSO_4$) and filtered over basic Al_2O_3 with THF–CH_2Cl_2 (1 : 49, v/v). The orange filtrate was concentrated to 3 mL, MeOH (50 mL) was added and the orange mixture was concentrated to 20 mL. After 1 h, the orange solid was isolated by centrifugation and dried *in vacuo*. Yield: 23 mg (94%). λ_{max}(CH_2Cl_2)/nm 416 (log ε 5.73), 528 (4.59); δ_H($CDCl_3$) 8.77 (6 H, m, β-H), 8.71 (2H, d, *J* 5.1, β-H), 7.99 (2 H, s, ArH_{pincer}), 7.89 (6 H, d, *J* 7.5, Ar$H_{p\text{-tol}}$), 7.48 (6 H, d, *J* 7.5, Ar$H_{p\text{-tol}}$), 3.78 (4 H, s, CH_2N), 2.65 (6 H, s, ArCH_3), 2.39 (12 H, s, N(CH_3)$_2$); δ_C($CDCl_3$) 143.0, 143.0, 142.9, 142.6, 139.6, 138.1, 137.5, 137.5, 134.8, 133.8, 133.7, 132.5, 132.3, 132.2, 131.8, 127.7, 127.1, 119.3, 119.2, 117.8, 64.4, 45.9, 21.6; MALDI-TOF MS (DHB): *m*/*z* 906.40 ($[M + H]^+$. $C_{53}H_{48}BrN_6Ni$ requires 906.24).

[5-(3,5-Bis[(dimethylamino)methyl]-4-bromidopalladio(II)-phenyl)-10,15,20-tris(*p*-tolyl)porphyrinato]nickel(II) ([Ni(PdBr)])

Route A: **[Ni(Br)]** (54.0 mg, 59.6 μmol) and $[Pd_2dba_3]\cdot CHCl_3$ (32 mg, 30.9 μmol) were dissolved in benzene (20 mL) and the dark red mixture was stirred at ambient temperature for 16 h. $HNEt_2$ (5 drops) and MeOH (1 mL) were then added and after 3 h, the mixture was filtered over Celite and the residue was washed with benzene (20 mL). The dark red filtrate was concentrated to 10 mL, hexanes (40 mL) were added and the solution was concentrated to approximately 30 mL and stored for 2 h at −30 °C. The formed dark orange precipitate was collected by centrifugation and sonicated with hexanes (40 mL) for 30 min and centrifuged again. The resulting orange solid was dried *in vacuo*. Yield: 56.0 mg (95%).

Route B: **[2H(PdBr)]** (36.8 mg, 38.5 μmol) was dissolved in CH_2Cl_2 (10 mL) and a saturated solution of $Ni(OAc)_2\cdot 4H_2O$ in MeOH (2 mL) was added under stirring. After 24 h at reflux temperature, the mixture was cooled to room temperature, extracted with H_2O (4 × 10 mL), and the organic layer was dried ($MgSO_4$), filtered, and concentrated to 5 mL. Addition of hexanes (30 mL) led to the full precipitation of the title compound as an orange solid. Yield: 29.7 mg (74%). Found: C 63.06, H 4.75,

N 8.21. Calcd for $C_{53}H_{47}BrN_6NiPd$: C 62.84, H 4.68, N 8.30%; $\lambda_{max}(CH_2Cl_2)$/nm 418 (log ε 5.74), 530 (4.62); $\delta_H(CDCl_3)$ 8.72 (8 H, m, β-H), 7.88 (6 H, m, Ar$H_{p\text{-tol}}$), 7.44 (6 H, m, Ar$H_{p\text{-tol}}$), 7.33 (2 H, s, ArH_{pincer}), 4.10 (4 H, s, CH_2N), 3.06 (12 H, s, N(CH_3)$_2$), 2.62 (6 H, s, ArCH_3), 2.60 (3 H, s, ArCH_3); $\delta_C(CDCl_3)$ 157.1, 143.6, 143.0, 143.0, 143.0, 142.9, 138.2, 137.7, 133.9, 133.8, 132.4, 132.3, 132.1, 127.8, 125.5, 119.3, 119.1, 74.8, 54.1, 21.7; MALDI-TOF MS (9NA): *m*/*z* 1011.66 ([M]$^+$. $C_{53}H_{47}BrN_6NiPd$ requires 1011.15), 933.48 ([M – Br]$^+$. $C_{53}H_{47}N_6NiPd$ requires 933.23).

[5-(3,5-Bis[(dimethylamino)methyl]-4-bromophenyl)-10,15,20-tris(*p*-tolyl)porphyrinato]zinc(II) ([Zn(Br)])

[2H(Br)] (76.0 mg, 89.4 μmol) was dissolved in dry CH_2Cl_2 and stirred at room temperature. Subsequently, a saturated solution of $Zn(OAc)_2{\cdot}2H_2O$ in degassed MeOH (2 mL, excess) was added and stirring was continued. After 30 min, degassed H_2O (40 mL), CH_2Cl_2 (20 mL), and K_2CO_3 (6 M, 2 mL) were added and the phases were separated. The organic layer was washed with brine (30 mL), dried ($MgSO_4$), filtered and loaded onto a silica gel column. Some contamination was eluted with CH_2Cl_2/hexanes (1 : 1, v/v) and the product with CH_2Cl_2/hexanes/THF (1 : 1 : 3, v/v/v) as a pink band. The volatiles were evaporated *in vacuo* and the purple residue was redissolved in CH_2Cl_2 (20 mL), hexanes (60 mL) were added and the solution was concentrated to 20 mL. The precipitated pink solid was collected by centrifugation and dried *in vacuo* to give the very insoluble title compound. Yield: 71 mg (89%). Found: C 68.70, H 5.75, N 8.36. Calcd for $C_{53}H_{49}BrN_6OZn$ ($C_{53}H_{47}BrN_6Zn{\cdot}H_2O$): C 68.35, H 5.30, N 9.02%; $\lambda_{max}(CH_2Cl_2)$/nm 424 (log ε 5.76), 553 (4.34), 597 (3.84); $\delta_H(CDCl_3$/1% pyridine-d_5) 8.86 (6 H, m, β-H), 8.80 (2 H, d, *J* 4.8, β-H), 8.16 (2 H, s, ArH_{pincer}), 8.06 (6 H, d, *J* 6.9, Ar$H_{p\text{-tol}}$), 7.50 (6 H, d, *J* 6.9, Ar$H_{p\text{-tol}}$), 3.84 (4 H, s, CH_2N), 2.68 (9 H, s, ArCH_3), 2.42 (12 H, s, N(CH_3)$_2$; δ_C(CDCl$_3$/1% pyridine-d_5) 150.4, 150.3, 150.0, 142.4, 140.8, 136.9, 136.7, 135.9, 134.7, 132.0, 131.8, 131.7, 131.3, 127.2, 126.9, 121.0, 120.8, 119.2. 64.5, 46.0, 21.7; LDI-TOF MS: *m*/*z* 912.35 (M$^+$. $C_{53}H_{47}BrN_6Zn$ requires 912.23).

[5-(3,5-Bis[(dimethylamino)methyl]-4-bromidopalladio(II)-phenyl)-10,15,20-tris(*p*-tolyl)porphyrinato]zinc(II) ([Zn(PdBr)])

Route A: **[Zn(Br)]** (66.0 mg, 72.3 μmol) was dissolved in a mixture of benzene (20 mL) and THF (10 mL) and stirred at ambient temperature. $[Pd_2dba_3]{\cdot}CHCl_3$ (43 mg, 41.5 μmol) was subsequently added and the dark red solution was subsequently stirred for 28 h. $HNEt_2$ (1 mL) and MeOH (1 mL) were then added and after 1 h, the mixture was filtered over Celite and the residue was washed with acetone/benzene (1 : 1, v/v, 30 mL). The dark pink filtrate was concentrated to 10 mL, hexanes (40 mL) were added and the solution was concentrated to approximately 30 mL. The formed purple precipitate was collected by centrifugation and sonicated with hexanes (40 mL) for 30 min and centrifuged again. The resulting purple solid was dried *in vacuo*. Yield: 67.8 mg (92%).

Route B: **[2H(PdBr)]** (36.6 mg, 38.3 μmol) was dissolved in CH_2Cl_2 (8 mL) and a saturated solution of $Zn(OAc)_2{\cdot}2H_2O$ in MeOH (2 mL) was added under stirring. After 2 h at ambient temperature, the mixture was extracted with H_2O (4 × 10 mL), dried ($MgSO_4$) and filtered. The pink solution was filtered over silica gel with THF–CH_2Cl_2 (1 : 2, v/v), the first band was collected and concentrated to 3 mL. Addition of hexanes (30 mL) led to the full precipitation of the title compound as a red solid. Yield: 32.8 mg (84%). Found: C 62.29, H 4.74, N 8.18. Calcd for $C_{53}H_{47}BrN_6PdZn$: C 62.43, H 4.65, N 8.24%; $\lambda_{max}(CH_2Cl_2)$/nm 422 (log ε 5.78), 549 (4.36), 590 (3.89); $\delta_H(CDCl_3$/1% pyridine-d_5) 8.89 (8 H, m, β-H), 8.07 (6 H, m, Ar$H_{p\text{-tol}}$), 7.50 (8 H, m, Ar$H_{p\text{-tol}}$ + ArH_{pincer}), 4.10 (4 H, s, CH_2N), 3.08 (12 H, s, N(CH_3)$_2$), 2.69 (6 H, s, ArCH_3), 2.67 (3 H, s, ArCH_3); δ_C(CDCl$_3$/1% pyridine-d_5) 156.4, 150.4, 150.4, 150.3, 150.2, 142.9, 140.8, 140.4, 136.9, 134.7, 131.8, 131.7, 131.5, 127.3, 126.5, 120.9, 120.8, 120.6, 74.8, 54.1, 21.7; MALDI-TOF MS (9NA): *m*/*z* 1021.09 ([M]$^+$. $C_{53}H_{47}BrN_6PdZn$ requires 1020.14).

5-(4-Aquapalladio(II)-3,5-bis[(dimethylamino)methyl]phenyl)-10,15,20-tris(*p*-tolyl)porphyrin ([2H(PdOH$_2$)]BF$_4$)

[2H(PdBr)] (27 mg, 28 μmol) was dissolved in dry CH_2Cl_2 (30 mL) and the dark red solution was stirred at ambient temperature while shielded from light. Upon addition of $AgBF_4$ (8 mg, 41 μmol) the mixture quickly turned green and after 5 min H_2O (1 drop) was added and the mixture was filtered over Celite. The residue was washed with acetone (20 mL) to give a green filtrate. All volatiles were evaporated and the remaining dark residue was washed extensively with H_2O (6 × 10 mL) on a plug of cotton. The latter was then extracted with acetone (10 mL) and the product mixture was precipitated with Et_2O (40 mL). The solid was re-dissolved in acetone (30 mL), filtered over Celite and *i*-Pr_2NEt (200 μL) was added, which restored the dark red colour of the free-base porphyrin. All volatiles were evaporated and the red solid was washed with hexanes (3 × 50 mL) and sonicated with demi H_2O (90 mL) for 1 h. The mixture was then again filtered over Celite and the residue was thoroughly washed with H_2O (3 × 50 mL). The desired complex was then washed off with acetone/MeOH (2 : 1, v/v, 3 × 50 mL) to give a pink filtrate, which was evaporated to dryness. Acetone (20 mL) was added and the resulting mixture was treated with hexanes to yield the title compound as a red solid, which was isolated by centrifugation and thoroughly dried *in vacuo*. Yield: 22 mg (79%). $\delta_H(CD_2Cl_2$/10% pyridine-d_5) 8.91 (4 H, s, β-H), 8.89 (4 H, s, β-H), 8.11 (6 H, m, Ar$H_{p\text{-tol}}$), 7.74 (2 H, s, ArH_{pincer}), 7.60 (6 H, m, Ar$H_{p\text{-tol}}$), 4.41 (4 H, s, CH_2N), 2.89 (12 H, s, N(CH_3)$_2$), 2.72 (6 H, s, ArCH_3), 2.67 (3 H, s, ArCH_3), –2.81 (2 H, s, NH); $\delta_F(CD_2Cl_2$/10% pyridine-d_5) –153; MALDI-TOF MS (9NA): *m*/*z* 876.00 ([M – H_2O – BF_4]$^+$. $C_{53}H_{49}N_6Pd$ requires 875.31).

[5-(4-Aquapalladio(II)-3,5-bis[(dimethylamino)methyl]phenyl)-10,15,20-tris(*p*-tolyl)porphyrinato]-magnesium(II) ([Mg(PdOH$_2$)]BF$_4$)

[Mg(PdCl)] (28 mg, 29 μmol) was dissolved in dry CH_2Cl_2 (25 mL), *i*-Pr_2NEt (700 μL) was added and the pink solution was stirred at ambient temperature while shielded from light. $AgBF_4$ (10 mg, 51 μmol) was subsequently added and after 5 min the mixture was filtered over Celite and the residue was washed with acetone (20 mL). The filtrate was evaporated to dryness and the remaining dark residue was washed with hexanes (3 × 50 mL) and sonicated with demi H_2O (90 mL) for 1 h. The mixture was then again filtered over Celite and the residue was thoroughly washed with demi H_2O (3 × 50 mL). The desired complex was then washed

off with acetone/MeOH (2 : 1, v/v, 3 × 50 mL) to give a pink filtrate, which was evaporated to dryness. Acetone (20 mL) was added and the resulting mixture was treated with hexanes to yield the title compound as a pink solid, which was isolated by centrifugation and thoroughly dried *in vacuo*. Yield: 22 mg (79%). $\delta_H(CD_2Cl_2/10\%$ pyridine-$d_5)$ 8.90 (8 H, m, β-H), 8.08 (6 H, m, Ar$H_{p\text{-tol}}$), 7.73 (2 H, s, ArH_{pincer}), 7.57 (6 H, m, Ar$H_{p\text{-tol}}$), 4.39 (4 H, s, CH_2N), 2.88 (12 H, s, N(CH_3)$_2$), 2.72 (6 H, s, ArCH_3), 2.71 (3 H, s, ArCH_3); $\delta_F(CD_2Cl_2/10\%$ pyridine-$d_5)$ −150; MALDI-TOF MS (9NA): m/z 896.43 ([M − H_2O − BF_4]$^+$. $C_{53}H_{47}N_6MgPd$ requires 897.28).

[5-(4-Aquapalladio(II)-3,5-bis[(dimethylamino)methyl]phenyl)-10,15,20-tris(*p*-tolyl)porphyrinato]-nickel(II) ([Ni(PdOH$_2$)]BF$_4$)

[Ni(PdBr)] (28.0 mg, 27.6 μmol) was dissolved in a mixture of CH_2Cl_2 (30 mL) and *i*-Pr_2NEt (500 μL) and the resulting orange solution was stirred at room temperature. $AgBF_4$ (11 mg, 56 μmol) was subsequently added followed by H_2O (2 drops) after 15 min. The mixture was subsequently filtered over Celite and the residue was washed with MeOH/acetone (1 : 1, v/v, 20 mL). The orange filtrate was evaporated to dryness and sonicated for 40 min with demi H_2O (40 mL). The mixture was filtered over a glass frit and the residue was thoroughly washed with H_2O (4 × 50 mL). The residue was subsequently extracted with acetone/MeOH (3 : 1, v/v, 2 × 30 mL) and all volatiles were evaporated *in vacuo*. The residue was solubilized in hot acetone (30 mL), hexanes (40 mL) were added, and the mixture was concentrated to 20 mL. The resulting red precipitate was collected by centrifugation and thoroughly dried *in vacuo*. Yield: 28 mg (98%). $\delta_H(CD_2Cl_2/10\%$ pyridine-$d_5)$ 8.85 (8 H, m, β-H), 7.92 (6 H, m, Ar$H_{p\text{-tol}}$), 7.55 (2 H, s, ArH_{pincer}), 7.54 (6 H, m, Ar$H_{p\text{-tol}}$), 4.36 (4 H, s, CH_2N), 2.85 (12 H, s, N(CH_3)$_2$), 2.67 (9 H, s, ArCH_3); $\delta_F(CD_2Cl_2/10\%$ pyridine-$d_5)$ −151; MALDI-TOF MS (9NA): m/z 933.64 ([M − H_2O − BF_4]$^+$. $C_{53}H_{47}N_6NiPd$ requires 933.23).

[5-(4-Aquapalladio(II)-3,5-bis[(dimethylamino)methyl]phenyl)-10,15,20-tris(*p*-tolyl)porphyrinato]-zinc(II) ([Zn(PdOH$_2$)]BF$_4$)

[Zn(PdBr)] (62 mg, 61 μmol) was dissolved in a mixture of CH_2Cl_2 (25 mL) and *i*-Pr_2NEt (1 mL) and the resulting pink solution was stirred at room temperature. $AgBF_4$ (20 mg, 102 μmol) was subsequently added followed by H_2O (2 drops) after 15 min. The mixture was subsequently filtered over Celite and the residue was washed with MeOH/acetone (1 : 1, v/v, 40 mL). The purple filtrate was evaporated to dryness and sonicated for 40 min with demi H_2O (40 mL). The mixture was filtered over a glass frit and the residue was thoroughly washed with H_2O (4 × 50 mL). The residue was subsequently extracted with acetone/MeOH (3 : 1, v/v, 3 × 50 mL) and all volatiles were evaporated *in vacuo*. The residue was solubilised in hot acetone (30 mL), hexanes (40 mL) were added, and the mixture was concentrated to 20 mL. The resulting red precipitate was collected by centrifugation and thoroughly dried *in vacuo*. Yield: 55 mg (86%). $\delta_H(CD_2Cl_2/10\%$ pyridine-$d_5)$ 8.87 (8 H, m, β-H), 8.09 (6 H, m, Ar$H_{p\text{-tol}}$), 7.73 (2 H, s, ArH_{pincer}), 7.60 (6 H, m, Ar$H_{p\text{-tol}}$), 4.52 (4 H, s, CH_2N), 2.97 (12 H, s, N(CH_3)$_2$), 2.70 (6 H, s, ArCH_3), 2.69 (3 H, s, ArCH_3); $\delta_F(CD_2Cl_2/10\%$ pyridine-$d_5)$ −152; MALDI-TOF MS (9NA): m/z 939.43 ([M − H_2O − BF_4]$^+$. $C_{53}H_{47}N_6PdZn$ requires 939.22).

5-(3,5-Bis[(dimethylamino)methyl]-4-chloridoplatino(II)-phenyl)-10,15,20-tris(*p*-tolyl)porphyrin ([2H(PtCl)])

[Pt_2dipdba$_3$] (374 mg, 278 μmol) was added to a degassed, dark red solution of **3** (438 mg, 515 μmol) in dry benzene (30 mL) and the dark purple solution was heated to reflux and stirred. The progress of the reaction was monitored by TLC (hexanes/THF, 1 : 1, v/v). After 5 h all Pt_2(dipdba)$_3$ had reacted but a bit of **3** was still visible. Another 35 mg of Pt_2(dipdba)$_3$ were added, the mixture was heated for another 60 min to reflux after which time the black solution was cooled RT and evaporated to dryness *in vacuo*. THF (30 mL) was added and the dark solution was stirred overnight and filtered over Celite to give a dark red solution. After concentration of the filtrate to 5 mL hexanes (60 mL) were added and the precipitate was collected by centrifugation after 16 h at −30 °C (514 mg). The compound was subsequently dissolved in CH_2Cl_2 (40 mL) and evaporated onto silica gel (20 g). The silica gel was poured on top of a silica gel column (prepared with 1% MeOH in CH_2Cl_2) and **[2H(PtBr)]** was eluted as the third band using a gradient of 1% MeOH to 3% MeOH. Yield: 480 mg (89%). Found: C 60.78, H 4.66, N 7.86. Calcd for $C_{53}H_{49}BrN_6Pt$: C 60.92, H 4.73, N 8.04%; $\lambda_{max}(CH_2Cl_2)$/nm 423 (log ε 5.76), 517 (4.42), 555 (4.14), 594 (3.97), 650 (3.84); $\delta_H(CDCl_3)$ 8.86 (8 H, m, β-H), 8.08 (6 H, d, *J* 7.8, Ar$H_{p\text{-tol}}$), 7.60 (2 H, s, ArH_{pincer}), 7.54 (6 H, d, *J* 7.8, Ar$H_{p\text{-tol}}$), 4.24 (4 H, s, CH_2N), 3.29 (12 H, s, N(CH_3)$_2$), 2.71 (6 H, s, ArCH_3), 2.70 (6 H, s, ArCH_3), −2.75 (2 H, s, NH); $\delta_C(CDCl_3)$ 145.9, 141.8, 139.4, 137.7, 137.5, 134.7, 134.6, 131.1 (b), 127.6, 126.2, 121.1, 120.3, 120.2, 77.7, 55.5, 21.7; $\delta_{Pt}(CDCl_3)$ −3196; MALDI-TOF MS (DHB): m/z 1044.00 ([M + H]$^+$. $C_{53}H_{50}BrN_6Pt$ requires 1044.29). This material was dissolved in dry CH_2Cl_2 (30 mL) and the dark red solution was stirred at ambient temperature while shielded from light. Upon addition of $AgBF_4$ (97.3 mg, 500 μmol) the mixture quickly turned green. After 5 min, brine (50 mL) was added and the mixture was vigorously stirred for 2 h. The layers were separated and the organic layer was dried ($MgSO_4$), filtered and concentrated to 20 mL. Addition of hexanes (60 mL) led to the precipitation of the title compound as a purple solid. Yield: 437 mg (95%). $\lambda_{max}(CH_2Cl_2)$/nm 423 (log ε 5.76), 517 (4.42), 555 (4.14), 594 (3.97), 650 (3.84); $\delta_H(CDCl_3)$ 8.86 (8 H, m, β-H), 8.08 (6 H, d, *J* 7.8, Ar$H_{p\text{-tol}}$), 7.60 (2 H, s, ArH_{pincer}), 7.55 (6 H, d, *J* 7.8, Ar$H_{p\text{-tol}}$), 4.25 (4 H, s, CH_2N), 3.26 (12 H, s, N(CH_3)$_2$), 2.71 (6 H, s, ArCH_3), 2.70 (6 H, s, ArCH_3), −2.75 (2 H, s, NH); $\delta_C(CDCl_3)$ 144.8, 141.8, 139.4, 137.6, 137.5, 134.7, 134.6, 131.1 (b), 127.6, 126.2, 121.1, 120.2 (2 ×), 78.0, 54.8, 21.7; $\delta_{Pt}(CDCl_3)$ −3181; MALDI-TOF MS (DHB): m/z 1001.23 ([M+H]$^+$. $C_{53}H_{50}ClN_6Pt$ requires 1000.55).

[5-(3,5-Bis[(dimethylamino)methyl]-4-chloridoplatino(II)-phenyl)-10,15,20-tris(*p*-tolyl)porphyrinato]-magnesium(II) ([Mg(PtCl)])

Route A: a suspension of **[Mg(Br)]** (42 mg, 48 μmol) and [Pt_2dipdba$_3$] (32 mg, 24 mmol) in dry benzene (10 mL) was treated with THF (3 mL) to give a clear solution. The dark solution was heated to reflux and stirring was continued for 3 h. The solution was allowed to cool down to ambient temperature, filtered over Celite and the filtrate was evaporated to dryness. The resulting greenish solid was sonicated with hexanes (70 mL) and isolated by centrifugation. It was re-dissolved in a mixture of CH_2Cl_2 (30 mL) and *i*-Pr_2NEt (1 mL), and subsequently treated with $AgBF_4$ (10 mg, 51 μmol). After 5 min of stirring at room temperature, the

mixture was diluted with brine (30 mL) and vigorously stirred for an additional 2 h. The layers were separated and the organic layer was dried ($MgSO_4$), filtered, and concentrated to 5 mL. Addition of hexanes (40 mL) followed by concentration of the mixture to 20 mL led to the precipitation of the title compound as a greenish solid, which was dried *in vacuo*. Yield: 45 mg (92%).

Route B: a solution of **[2H(PtCl)]** (30 mg, 30 μmol) in dry CH_2Cl_2 (30 mL) was treated with *i*-Pr_2NEt (1 mL) and $MgBr_2{\cdot}OEt_2$ (500 mg, 1.94 mmol) and the mixture was stirred overnight at ambient temperature. The resulting pink solution was washed with 5% $NaHCO_3$ (3 × 50 mL) and brine (2 × 50 mL) and loaded onto a column with alumina. The desired product was eluted with MeOH–CH_2Cl_2 (1 : 9, v/v). The volatiles were evaporated and the resulting solid was re-dissolved in CH_2Cl_2 (10 mL). Hexanes (60 mL) were added and the mixture was concentrated to 30 mL and the resulting greenish solid was isolated by means of centrifugation. Yield: 22 mg (72%).

Found: C 59.95, H 5.00, N 6.65. Calcd for $C_{60}H_{65}Cl_3MgN_6OPt$ ($C_{53}H_{47}ClMgN_6Pt{\cdot}CH_2Cl_2{\cdot}H_2O{\cdot}C_6H_{14}$): C 59.46, H 5.41, N 6.93%; $\lambda_{max}(CH_2Cl_2)$/nm 430 (log ε 5.80), 566 (4.38), 608 (4.26); $\delta_H(CDCl_3$/1% pyridine-d_5) 8.91 (2 H, d, *J* 4.0, β-H), 8.80 (6 H, m, β-H), 8.06 (6 H, d, *J* 7.6, Ar$H_{p\text{-tol}}$), 7.56 (8 H, m, ArH_{pincer} + Ar$H_{p\text{-tol}}$), 4.28 (4 H, s, CH_2N), 3.17 (12 H, s, N(CH_3)$_2$), 2.67 (9 H, s, ArCH_3); $\delta_C(CDCl_3$/1% pyridine-d_5) 153.4, 150.3, 150.2, 150.2, 150.1, 142.0, 141.2, 138.6, 136.8, 134.6, 134.6, 132.5, 131.6, 131.6, 131.4, 127.2, 126.0, 121.5, 121.3, 76.3, 54.0, 20.8; $\delta_{Pt}(CDCl_3$/1% pyridine-d_5) −3195; MALDI-TOF MS (9NA): *m*/*z* 1021.93 ([M]$^+$. $C_{53}H_{47}ClMgN_6Pt$ requires 1022.30).

[5-(3,5-Bis[(dimethylamino)methyl]-4-chloridoplatino(II)-phenyl)-10,15,20-tris(*p*-tolyl)porphyrinato]nickel(II) ([Ni(PtCl)])

Route A: **[Ni(Br)]** (22 mg, 24 μmol) was dissolved in dry benzene (5 mL), [Pt_2dipdba$_3$] (16.1 mg, 12 μmol) was added, and the dark red solution was heated to reflux for 12 h. After cooling to ambient temperature, the mixture was filtered over Celite and the residue was washed with benzene/acetone (1 : 1, 20 mL). The orange filtrate was concentrated to 5 mL and hexanes (20 mL) were subsequently added to precipitate the crude product **[Ni(PtX)]** (X = Br, Cl) as an orange solid. The solid was dissolved in dry CH_2Cl_2 (30 mL) and *i*-Pr_2NEt (1 mL, excess) was added to give an orange solution, which was stirred at ambient temperature. $AgBF_4$ (5 mg, 26 μmol) was subsequently added followed after 5 min by brine (30 mL) and the mixture was vigorously stirred for 1 h. The organic layer was isolated, dried ($MgSO_4$), filtered and loaded onto a silica gel column (CH_2Cl_2). The desired product was eluted with MeOH–CH_2Cl_2 (1 : 19, v/v) as an orange band, which was concentrated to 5 mL and diluted with hexanes (80 mL) to give an orange solid, which was isolated by centrifugation. Yield: 23 mg (91%).

Route B: **[2H(PtCl)]** (23 mg, 23 μmol) was dissolved in degassed $CHCl_3$ (6 mL) and the dark red solution was treated with a saturated solution of $Ni(OAc)_2{\cdot}4H_2O$ in MeOH (1 mL) and the resulting mixture was heated to reflux overnight. After cooling to room temperature, the orange mixture was extracted with H_2O (4 × 20 mL) and washed with brine (20 mL). The organic layer was dried ($MgSO_4$), loaded onto a silica gel column and the product was eluted with MeOH–CH_2Cl_2 (1 : 19, v/v) as an orange band, which was concentrated to 5 mL and diluted with hexanes (80 mL) to give an orange solid, which was isolated by centrifugation. Yield: 16 mg (67%). Found: C 59.95, H 5.00, N 6.65. Calcd for $C_{60}H_{65}Cl_3MgN_6OPt$ ($C_{53}H_{47}ClMgN_6Pt{\cdot}CH_2Cl_2{\cdot}H_2O{\cdot}C_6H_{14}$): C 59.46, H 5.41, N 6.93%; $\lambda_{max}(CH_2Cl_2)$/nm 430 (log ε 5.80), 566 (4.38), 608 (4.26); $\delta_H(CDCl_3)$ 8.80 (2 H, d, *J* 5.2, β-H), 8.76 (6 H, m, β-H), 7.89 (6 H, d, *J* 8.0, Ar$H_{p\text{-tol}}$), 7.46 (6 H, d, *J* 8.0, Ar$H_{p\text{-tol}}$), 7.39 (2 H, s, ArH_{pincer}), 4.21 (4 H, s, CH_2N), 3.23 (12 H, s, N(CH_3)$_2$), 2.64 (6 H, s, ArCH_3), 2.63 (3 H, s, ArCH_3); $\delta_C(CDCl_3)$ 153.4, 150.3, 150.2, 150.2, 150.1, 142.0, 141.2, 138.6, 136.8, 134.6, 134.6, 132.5, 131.6, 131.6, 131.4, 127.2, 126.0, 121.5, 121.3, 76.3, 54.0, 20.8; $\delta_{Pt}(CDCl_3)$ −3183; MALDI-TOF MS (DHB): *m*/*z* 1056.27 (M$^+$. $C_{53}H_{47}ClN_6NiPt$ requires 1056.26), 1021.27 ([M − Cl]$^+$. $C_{53}H_{47}N_6NiPt$ requires 1021.29), 825.30 ([M − PtCl]$^+$. $C_{53}H_{47}N_6Ni$ requires 825.32).

[5-(3,5-Bis[(dimethylamino)methyl]-4-chloridoplatino(II)-phenyl)-10,15,20-tris(*p*-tolyl)porphyrinato]-zinc(II) ([Zn(PtCl)])

Route A: **[Zn(Br)]** (40 mg, 44 μmol) was dissolved in dry benzene (5 mL), [Pt_2dipdba$_3$] (32 mg, 24 μmol) was added, and the dark red solution was heated to reflux for 16 h. After cooling to ambient temperature, the mixture was filtered over Celite and the residue was washed with benzene/acetone (1 : 1, v/v, 20 mL). The red filtrate was concentrated to 5 mL and hexanes (20 mL) were subsequently added to precipitate the crude product **[Zn(PtX)]** (X = Br, Cl) as a purple/green solid. The solid was dissolved in dry CH_2Cl_2 (30 mL) and *i*-Pr_2NEt (1 mL, excess) was added to give a pink solution, which was stirred at ambient temperature. $AgBF_4$ (10 mg, 52 μmol) was subsequently added followed after 5 min by brine (30 mL) and the mixture was vigorously stirred for 1 h. The organic layer was isolated, dried ($MgSO_4$), filtered and loaded onto a silica gel column (CH_2Cl_2). The desired product was eluted with MeOH–CH_2Cl_2 (1 : 9, v/v) as a pink band, which was concentrated to 5 mL and diluted with hexanes (80 mL) to give the product as a green/purple solid, which was isolated by centrifugation. Yield: 41 mg (88%).

Route B: **[2H(PtCl)]** (30 mg, 30 μmol) was dissolved in degassed $CHCl_3$ (10 mL) and the dark red solution was treated with a saturated solution of $Zn(OAc)_2{\cdot}2H_2O$ in MeOH (1 mL) and the resulting mixture was stirred at room temperature for 20 min. The pink mixture was extracted with H_2O (2 × 20 mL) and washed with brine (20 mL). The organic layer was dried ($MgSO_4$), loaded onto a silica gel column and the product was eluted with MeOH–CH_2Cl_2 (1 : 19, v/v) as a pink band, which was concentrated to 5 mL and diluted with hexanes (80 mL) to give an purple/greenish solid, which was isolated by centrifugation. Yield: 23 mg (72%). Found: C 59.95, H 5.00, N 6.65. Calcd for $C_{60}H_{65}Cl_3MgN_6OPt$: C 59.46, H 5.41, N 6.93%; $\lambda_{max}(CH_2Cl_2)$/nm 430 (log ε 5.80), 566 (4.38), 608 (4.26); $\delta_H(CDCl_3)$ 9.01 (2 H, d, *J* 4.4, β-H), 8.96 (6 H, m, β-H), 8.09 (6 H, d, *J* 7.6, Ar$H_{p\text{-tol}}$), 7.63 (2 H, s, ArH_{pincer}), 7.55 (6 H, d, *J* 7.6, Ar$H_{p\text{-tol}}$), 4.28 (4 H, s, CH_2N), 3.28 (12 H, s, N(CH_3)$_2$), 2.71 (6 H, s, ArCH_3), 2.70 (3 H, s, ArCH_3); $\delta_C(CDCl_3)$ 150.6, 150.5, 150.5, 150.4, 144.5, 141.6, 140.5, 138.2, 137.3, 134.5, 132.1, 131.9, 127.4, 126.0, 122.2, 121.3, 121.2, 78.1, 54.9, 21.7; $\delta_{Pt}(CDCl_3)$ −3189; MALDI-TOF MS (DHB): *m*/*z* 1062.58 (M$^+$. $C_{53}H_{47}ClN_6PtZn$ requires 1062.25), 1027.29 ([M − Cl]$^+$. $C_{53}H_{47}N_6PtZn$ requires 1027.28), 831.38 ([M − PtCl]$^+$. $C_{53}H_{47}N_6Zn$ requires 831.32).

Double Michael addition. A flame-dried vial was charged with the appropriate Pd catalyst (8.0 μmol) and dry CH_2Cl_2 (5.0 mL)

was added. After 15 min of stirring at 20 °C, ethyl α-cyanoacetate (170 μL, 1.60 mmol) was added which led to quick dissolution of all solids. Methyl vinyl ketone (390 μL, 4.80 mmol) was subsequently added, followed by *i*-Pr_2NEt (28 μL, 0.16 mmol) and the reaction mixture was stirred in the dark. Samples (100 μL) were taken at appropriate time intervals, and the CH_2Cl_2 and methyl vinyl ketone were quickly removed with a gentle stream of nitrogen (approximately 20 s). The samples were subsequently analysed by ^{1}H NMR spectroscopy and the conversions were determined by comparison of the signal intensities of the ethyl CH_2 protons (δ = 4.28 ppm) with the CH_2 protons of ethyl α-cyanoacetate (δ = 3.45 ppm).

X-Ray crystal structure determination of compound {[Mg(Br)](THF)$_2$}

$C_{61}H_{62.82}Br_{1.18}MgN_6O_2$ + disordered solvent, FW = 1030.99‡, purple plate, 0.30 × 0.12 × 0.03 mm^3, triclinic, $P\bar{1}$ (no. 2), a = 9.6539(12), b = 10.7179(12), c = 28.370(4) Å, α = 92.826(12), β = 99.512(11), γ = 90.753(17)°, V = 2890.9(6) Å^3, Z = 2, D_x = 1.184 g cm^{-3}‡, μ = 0.90 mm^{-1}‡. 35 693 reflections were measured on a Nonius Kappa CCD diffractometer with rotating anode (graphite monochromator, λ = 0.71073 Å) at a temperature of 150 K up to a resolution of $(\sin\theta/\lambda)_{max}$=0.59 Å^{-1}. Intensities were integrated with HKL2000.[111] The reflections were corrected for absorption on the basis of multiple measured reflections using the MULABS routine of the program PLATON[112] (0.78–0.97 correction range). 9890 Reflections were unique (R_{int}=0.0732). The structure was solved with the program SHELXS-86[113] using Direct Methods. The crystal structure contains voids (248 Å^3 per unit cell) filled with disordered solvent molecules. Their contribution to the structure factors was secured by back-Fourier transformation using the routine SQUEEZE of the program PLATON,[112] resulting in 55 electrons/unit cell. Residual electron density indicated the presence of the bromine substituted starting material, which was included in the refinement with partial occupancy. The structure was refined with SHELXL-97[114] against F^2 of all reflections. Most non-hydrogen atoms were refined with anisotropic displacement parameters. Hydrogen atoms were introduced in calculated positions and refined with a riding model. One tolyl and one THF moiety were refined with disorder models, respectively. 637 Parameters were refined with 51 restraints. R1/wR2 [$I > 2\sigma(I)$]: 0.0842/0.2145. R_1/wR_2 [all reflections]: 0.1335/0.2381. S = 1.039. Residual electron density between −0.48 and 0.72 e/Å^3. Geometry calculations and checking for higher symmetry was performed with the PLATON program.[112]

Acknowledgements

We thank The Netherlands Organisation for Scientific Research for a Jonge Chemici scholarship (B. M. J. M. S. and R. J. M. K. G.).

Notes and references

1 M. Albrecht and G. van Koten, *Angew. Chem., Int. Ed.*, 2001, **40**, 3750–3781.
2 J. Kjellgren, H. Sundén and K. J. Szabó, *J. Am. Chem. Soc.*, 2004, **126**, 474–475.
3 V. J. Olsson, S. Sebelius, N. Selander and K. J. Szabó, *J. Am. Chem. Soc.*, 2006, **128**, 4588–4589.
4 S. Sebelius, V. J. Olsson, O. A. Wallner and K. J. Szabó, *J. Am. Chem. Soc.*, 2006, **128**, 8150.
5 N. Selander, S. Sebelius, C. Estay and K. J. Szabó, *Eur. J. Org. Chem.*, 2006, 4085–4087.
6 J. T. Singleton, *Tetrahedron*, 2003, **59**, 1837–1857.
7 N. Solin, J. Kjellgren and K. J. Szabó, *Angew. Chem., Int. Ed.*, 2003, **42**, 3656–3658.
8 N. Solin, J. Kjellgren and K. J. Szabó, *J. Am. Chem. Soc.*, 2004, **126**, 7026–7033.
9 M. E. Van Der Boom and D. Milstein, *Chem. Rev.*, 2003, **103**, 1759–1792.
10 O. A. Wallner and K. J. Szabó, *Org. Lett.*, 2004, **6**, 1829–1831.
11 O. A. Wallner and K. J. Szabó, *J. Org. Chem.*, 2005, **70**, 9215–9221.
12 W. C. Yount, H. Juwarker and S. L. Craig, *J. Am. Chem. Soc.*, 2003, **125**, 15302–15303.
13 J. M. Pollino and M. Weck, *Chem. Soc. Rev.*, 2005, **34**, 193–207.
14 H. P. Dijkstra, A. Chuchuryukin, B. M. J. M. Suijkerbuijk, G. P. M. van Klink, A. M. Mills, A. L. Spek and G. van Koten, *Adv. Synth. Catal.*, 2002, **344**, 771–780.
15 A. V. Chuchuryukin, H. P. Dijkstra, B. M. J. M. Suijkerbuijk, R. J. M. Klein Gebbink, G. P. M. van Klink, A. M. Mills, A. L. Spek and G. van Koten, *Angew. Chem., Int. Ed.*, 2003, **42**, 228–230.
16 A. V. Chuchuryukin, P. A. Chase, H. P. Dijkstra, B. M. J. M. Suijkerbuijk, A. M. Mills, A. L. Spek, G. P. M. van Klink and G. van Koten, *Adv. Synth. Catal.*, 2005, **347**, 447–462.
17 W. T. S. Huck, L. J. Prins, R. H. Fokkens, N. M. M. Nibbering, F. C. J. M. van Veggel and D. N. Reinhoudt, *J. Am. Chem. Soc.*, 1998, **120**, 6240–6246.
18 W. T. S. Huck, F. C. J. M. van Veggel and D. N. Reinhoudt, *Angew. Chem., Int. Ed. Engl.*, 1996, **35**, 1213–1215.
19 G. van Koten, *Pure Appl. Chem.*, 1989, **61**, 1681–1694.
20 M. Albrecht, R. A. Gossage, M. Lutz, A. L. Spek and G. van Koten, *Chem.–Eur. J.*, 2000, **6**, 1431–1445.
21 M. Albrecht, M. Lutz, A. L. Spek and G. van Koten, *Nature*, 2000, **406**, 970–974.
22 M. Albrecht, G. Rodríguez, J. Schoenmaker and G. van Koten, *Org. Lett.*, 2000, **2**, 3461–3464.
23 D. Beccati, K. M. Halkes, G. D. Batema, G. Guillena, A. Carvalho de Souza, G. van Koten and J. P. Kamerling, *ChemBioChem*, 2005, **6**, 1196–1203.
24 L. A. van de Kuil, H. Luitjes, D. M. Grove, J. W. Zwikker, J. G. M. Van Der Linden, A. M. Roelofsen, L. W. Jenneskens, W. Drenth and G. van Koten, *Organometallics*, 1994, **13**, 468–477.
25 M. Q. Slagt, G. Rodríguez, M. M. P. Grutters, R. J. M. Klein Gebbink, W. Klopper, L. W. Jenneskens, M. Lutz, A. L. Spek and G. van Koten, *Chem.–Eur. J.*, 2004, **10**, 1331–1344.
26 M. Tromp, J. A. van Bokhoven, M. Q. Slagt, R. J. M. Klein Gebbink, G. van Koten, D. E. Ramaker and D. C. Koningsberger, *J. Am. Chem. Soc.*, 2004, **126**, 4090–4091.
27 I. Göttker-Schnetmann and M. Brookhart, *J. Am. Chem. Soc.*, 2004, **126**, 9330–9338.
28 I. Göttker-Schnetmann, P. White and M. Brookhart, *J. Am. Chem. Soc.*, 2004, **126**, 1804–1811.
29 J. Aydin, N. Selander and Szabó, *Tetrahedron Lett.*, 2006, **47**, 8999–9001.
30 J. S. Fossey and C. J. Richards, *Organometallics*, 2004, **23**, 367–373.
31 B. M. J. M. Suijkerbuijk, L. Shu, R. J. M. Klein Gebbink, A. D. Schlüter and G. van Koten, *Organometallics*, 2003, **22**, 4175–4177.
32 B. M. J. M. Suijkerbuijk, M. Q. Slagt, R. J. M. Klein Gebbink, M. Lutz, A. L. Spek and G. van Koten, *Tetrahedron Lett.*, 2002, **43**, 6565–6568.
33 H. P. Dijkstra, C. A. Kruithof, N. Ronde, R. van de Coevering, D. J. Ramón, D. Vogt, G. P. M. van Klink and G. van Koten, *J. Org. Chem.*, 2003, **68**, 675–685.
34 H. P. Dijkstra, M. D. Meijer, J. Patel, R. Kreiter, G. P. M. van Klink, M. Lutz, A. L. Spek, A. J. Canty and G. van Koten, *Organometallics*, 2001, **20**, 3159–3168.
35 H. P. Dijkstra, P. Steenwinkel, D. M. Grove, M. Lutz, A. L. Spek and G. van Koten, *Angew. Chem., Int. Ed.*, 1999, **38**, 2185–2187.
36 D. E. Bergbreiter, P. L. Osburn, A. Wilson and E. M. Sink, *J. Am. Chem. Soc.*, 2000, **122**, 9058–9064.

‡ The derived parameters do not contain the contribution of the disordered solvent.

37 W. T. S. Huck, F. C. J. M. van Veggel, B. L. Kropman, D. H. A. Blank, E. G. Keim, M. M. A. Smithers and D. N. Reinhoudt, *J. Am. Chem. Soc.*, 1995, **117**, 8293–8294.
38 J. M. Pollino, L. P. Stubbs and M. Weck, *Macromolecules*, 2003, **36**, 2230–2234.
39 J. M. Pollino, L. P. Stubbs and M. Weck, *J. Am. Chem. Soc.*, 2004, **126**, 563–567.
40 J. M. Pollino and M. Weck, *Synthesis*, 2002, 1277–1285.
41 A. W. Kleij, R. A. Gossage, J. T. B. H. Jastrzebski, J. Boersma and G. van Koten, *Angew. Chem., Int. Ed.*, 2000, **39**, 176–178.
42 A. W. Kleij, R. A. Gossage, R. J. M. Klein Gebbink, N. Brinkmann, E. J. Reijerse, U. Kragl, M. Lutz, A. L. Spek and G. van Koten, *J. Am. Chem. Soc.*, 2000, **122**, 12112–12124.
43 A. Friggeri, H.-J. van Manen, T. Auletta, X.-M. Li, S. Zapotoczny, H. Schönherr, G. J. Vancso, J. Huskens, F. C. J. M. van Veggel and D. N. Reinhoudt, *J. Am. Chem. Soc.*, 2001, **123**, 6388–6395.
44 H.-J. van Manen, R. H. Fokkens, F. C. J. M. van Veggel and D. N. Reinhoudt, *Eur. J. Org. Chem.*, 2002, 3189–3197.
45 J. W. J. Knapen, A. W. Van Der Made, J. C. de Wilde, P. W. N. M. van Leeuwen, P. Wijkens, D. M. Grove and G. van Koten, *Nature*, 1994, **372**, 659–665.
46 M. D. Meijer, N. Ronde, D. Vogt, G. P. M. van Klink and G. van Koten, *Organometallics*, 2001, **20**, 3993–4000.
47 R. van de Coevering, M. Kuil, R. J. M. Klein Gebbink and G. van Koten, *Chem. Commun.*, 2002, 1636–1637.
48 N. C. Mehendale, J. R. A. Sietsma, K. P. de Jong, C. A. van Walree, R. J. M. Klein Gebbink and G. van Koten, *Adv. Synth. Catal.*, 2007, **349**, 2619–2630.
49 P. O'Leary, C. A. van Walree, N. C. Mehendale, J. Sumerel, D. E. Morse, W. C. Kaska, G. van Koten and R. J. M. Klein Gebbink, *Dalton Trans.*, 2009, 4289–4291.
50 S. A. Bonnet, J. Li, M. A. Siegler, L. S. von Chrzanowski, A. L. Spek, G. van Koten and R. J. M. Klein Gebbink, *Chem.–Eur. J.*, 2009, **15**, 3340–3343.
51 S. A. Bonnet, M. Lutz, A. L. Spek, G. van Koten and R. J. M. Klein Gebbink, *Organometallics*, 2008, **27**, 159–162.
52 S. A. Bonnet, J. H. van Lenthe, M. A. Siegler, A. L. Spek, G. van Koten and R. J. M. Klein Gebbink, *Organometallics*, 2009, **28**, 2325–2333.
53 M. Q. Slagt, R. J. M. Klein Gebbink, M. Lutz, A. L. Spek and G. van Koten, *J. Chem. Soc., Dalton Trans.*, 2002, 2591–2592.
54 M. Gagliardo, D. J. M. Snelders, P. A. Chase, R. J. M. Klein Gebbink, G. P. M. van Klink and G. van Koten, *Angew. Chem., Int. Ed.*, 2007, **46**, 8558–8573.
55 D. Dolphin, *The Porphyrins*, Academic Press, Inc., New York, 1978.
56 K. M. Smith, *Porphyrins and Metalloporphyrins*, Elsevier Scientific Publishing Company, Amsterdam, 1975.
57 M. Gouterman, in *The Porphyrins*, ed. D. Dolphin, Academic Press, Inc., New York, Editon edn, 1978, vol. 3.
58 J. W. Buchler, *Static Coordination Chemistry of Metalloporphyrins*, Elsevier Scientific Publishing Company, Amsterdam, 1975.
59 B. M. J. M. Suijkerbuijk, D. M. Tooke, M. Lutz, A. L. Spek, L. W. Jenneskens, G. van Koten and R. J. M. Klein Gebbink, *J. Org. Chem.*, 2010, **75**, 1534–1549.
60 B. M. J. M. Suijkerbuijk, S. D. Herreras Mártinez, G. van Koten and R. J. M. Klein Gebbink, *Organometallics*, 2008, **27**, 534–542.
61 A. D. Adler, F. R. Longo, J. D. Finarelli, J. Goldmacher, J. Assour and L. Korsakoff, *J. Org. Chem.*, 1967, **32**, 476.
62 B. M. J. M. Suijkerbuijk, M. Lutz, A. L. Spek, G. van Koten and R. J. M. Klein Gebbink, *Org. Lett.*, 2004, **6**, 3023–3026.
63 T. R. Janson and J. J. Katz, in *The Porphyrins*, ed. D. Dolphin, Academic Press, Inc. Ltd., London, Editon edn, 1979.
64 N. Jux, *Org. Lett.*, 2000, **2**, 2129–2132.
65 J. S. Lindsey and J. N. Woodford, *Inorg. Chem.*, 1995, **34**, 1063–1069.
66 K. Padmaja, L. Wei, J. S. Lindsey and D. F. Bocian, *J. Org. Chem.*, 2005, **70**, 7972–7978.
67 K. M. Kadish and L. R. Shiue, *Inorg. Chem.*, 1982, **21**, 1112–1115.
68 C. B. Storm, A. H. Corwin, R. R. Arellano, M. Martz and R. Weintraub, *J. Am. Chem. Soc.*, 1966, **88**, 2525–2532.
69 A. Satake and Y. Kobuke, *Tetrahedron*, 2005, **61**, 13–41.
70 V. McKee and G. A. Rodley, *Inorg. Chim. Acta*, 1988, **151**, 233–236.
71 G. Wu, A. Wong and S. Wang, *Can. J. Chem.*, 2003, **81**, 275–283.
72 V. McKee, C. C. Ong and G. A. Rodley, *Inorg. Chem.*, 1984, **23**, 4242.
73 J. A. Shelnutt, X.-Z. Song, J.-G. Ma, W. Jentzen and C. J. Medforth, *Chem. Soc. Rev.*, 1998, **27**, 31–41.
74 J. R. L. Priqueler, I. S. Butler and F. D. Rochon, *Appl. Spectrosc. Rev.*, 2006, **41**, 185–226.
75 Also the redox potentials of tetraphenylporphyrin complexes of 2H, Ni, Zn, and Mg follow this order, *viz.* $E_{1/2}(0/1) = 0.97, 0.95, 0.71, 0.54$ V, respectively (ref. 76).
76 J.-H. Fuhrhop, in *Porphyrins and Metalloporphyrins*, ed. K. M. Smith, Elsevier Scientific Publishing Company, Amsterdam, Editon edn, 1975, pp. 601–603.
77 Prior to each measurement the chemical shift value was referenced to 1M Na_2PtCl_6 in D_2O. In the original report by Slagt *et al.*, another reference compound (H_2PtCl_4) was used which leads to values 1191 ppm downfield of the values used in this chapter. The spread of data points around the best linear fit through them ($R = 0.974$) is significant. The experimental value for the Pt chemical shift therefore does not completely coincide with the theoretical value.
78 C. Hansch, A. Leo and R. W. Taft, *Chem. Rev.*, 1991, **91**, 165–195.
79 M. A. Stark, G. Jones and C. J. Richards, *Organometallics*, 2000, **19**, 1282–1291.
80 M. A. Stark and C. J. Richards, *Tetrahedron Lett.*, 1997, **38**, 5881–5884.
81 H. P. Dijkstra, M. Q. Slagt, A. McDonald, C. A. Kruithof, R. Kreiter, A. M. Mills, M. Lutz, A. L. Spek, W. Klopper, G. P. M. van Klink and G. van Koten, *Eur. J. Inorg. Chem.*, 2003, 830–838.
82 J. S. Fossey and C. J. Richards, *Organometallics*, 2002, **21**, 5259–5264.
83 M. Q. Slagt, S.-E. Stiriba, R. J. M. Klein Gebbink, H. Kautz, H. Frey and G. van Koten, *Macromolecules*, 2002, **35**, 5734–5737.
84 K. Takenaka and Y. Uozumi, *Org. Lett.*, 2004, **6**, 1833–1835.
85 The cationic products were much less mobile than the starting materials in a mixture of methanol and dichloromethane (1 : 9, v/v). In each case, the product was observed as a single spot.
86 H. P. Dijkstra, N. Ronde, G. P. M. van Klink, D. Vogt and G. van Koten, *Adv. Synth. Catal.*, 2003, **345**, 364–369.
87 D. M. Grove, G. van Koten, J. N. Louwen, J. G. Noltes, A. L. Spek and H. J. C. Ubbels, *J. Am. Chem. Soc.*, 1982, **104**, 6609–6616.
88 T. Ozawa and A. Hanaki, *J. Chem. Soc., Dalton Trans.*, 1985, 1513–1516.
89 G. Lipiner, I. Willner and Z. Aizenshtat, *Nouv. J. Chim.*, 1986, **10**, 91–92.
90 J. A. Johnson and D. A. Evans, *Acc. Chem. Res.*, 2000, **33**, 325–335.
91 M. Sawamura, M. Sudoh and Y. Ito, *J. Am. Chem. Soc.*, 1996, **118**, 3309–3310.
92 G. M. Sammis, H. Danjo and E. N. Jacobsen, *J. Am. Chem. Soc.*, 2004, **126**, 9928–9929.
93 S. Jautze and R. Peters, *Angew. Chem., Int. Ed.*, 2008, **47**, 9284–9288.
94 E. K. Van Den Beuken and B. L. Feringa, *Tetrahedron*, 1998, **54**, 12985–13011.
95 R. Breinbauer and E. N. Jacobsen, *Angew. Chem., Int. Ed.*, 2000, **39**, 3604–3607.
96 R. G. Konsler, J. Karl and E. N. Jacobsen, *J. Am. Chem. Soc.*, 1998, **120**, 10780–10781.
97 J. E. Huheey, E. A. Keiter and R. L. Keiter, *Inorganic Chemistry: Principles of Structure and Reactivity*, Harper Collins College Publishers, New York, 1993.
98 R. G. Pearson, *Chemical Hardness*, Wiley-VCH, Verlag GmbH, Weinheim, 1997.
99 M. H. Chisholm, J. Gallucci and K. Phomphrai, *Inorg. Chem.*, 2002, **41**, 2785–2794.
100 M. H. Chisholm, J. Gallucci and K. Phomphrai, *Inorg. Chem.*, 2005, **44**, 8004–8010.
101 T. Dudev, J. A. Cowan and C. Lim, *J. Am. Chem. Soc.*, 1999, **121**, 7665–7673.
102 G. Proni, G. Pescitelli, X. Huang, K. Nakanishi and N. Berova, *J. Am. Chem. Soc.*, 2003, **125**, 12914–12927.
103 J. V. Nardo and J. H. Dawson, *Inorg. Chim. Acta*, 1986, **123**, 9–13.
104 J. M. Lintuluoto, V. V. Borovkov and Y. Inoue, *J. Am. Chem. Soc.*, 2002, **124**, 13676–13677.
105 T. V. Duncan, I. V. Rubtsov, H. T. Uyeda and M. J. Therien, *J. Am. Chem. Soc.*, 2004, **126**, 9474–9475.
106 H. T. Uyeda, Y. Zhao, K. Wostyn, I. Asselberghs, K. Clays, A. Persoons and M. J. Therien, *J. Am. Chem. Soc.*, 2002, **124**, 13806–13813.

107 V. S.-Y. Lin, S. G. DiMagno and M. J. Therien, *Science*, 1994, **264**, 1105–1111.
108 S. Komiya, *Synthesis of Organometallic Compounds*, Wiley, Winchester, 1997.
109 A. Keasey, B. E. Mann, A. Yates and P. M. Maitlis, *J. Organomet. Chem.*, 1978, **152**, 117–123.
110 S. J. Shaw, S. Shanmugaathasan, O. J. Clarke, R. W. Boyle, A. G. Osborne and C. E. Edwards, *J. Porphyrins Phthalocyanines*, 2001, **5**, 575–581.
111 Z. Otwinowski and W. Minor, in *Methods in Enzymology*, Academic Press, New York, Editon edn, 1997, vol. 276, pp. 307–326.
112 A. L. Spek, *J. Appl. Crystallogr.*, 2003, **36**, 7–13.
113 G. M. Sheldrick, *SHELXS-86*, University of Göttingen, Germany, 1986.
114 G. M. Sheldrick, *SHELXL-97*, University of Göttingen, Germany, 1997.
115 B. M. J. M. Suijkerbuijk, D. M. Tooke, A. L. Spek, G. van Koten and R. J. M. Klein Gebbink, *Chem.–Asian J.*, 2007, **2**, 889–903.

